Neutron detection in a wide energy range: new detection materials and solutions

V.Mechinsky[1], A. Bondarev[1], E. Borisevich[1], A. Fedorov[1], I. Komendo[2], M. Korzhik[1], K. Okhotnikova[1], A. Timoshchenko[3]

[1] Institute for Nuclear Problems of Belarus State University, Minsk, Belarus
[2] National Research Center Kurchatov Institute, Moscow, Russia
[3]Physics Department, Belarus State University, Minsk, Belarus

The XVI-th International School-Conference "The Actual Problems of Microworld Physics"
Minsk, Belarus, 24 – 31 August, 2025

Main reactions for thermal neutrons detection

$^{3}He(n,p)^{3}H + 764$ keV (σ_T=5327 b)

$^{6}Li(n,\alpha)^{3}H + 4786$ keV (σ_T=945 b), ^{6}Li – 7.45% in natur. Li

$^{10}B(n,\alpha)^{7}Li + 2757$ keV (σ_T=3837 b), ^{10}B – 20% in natur. B

$^{155}Gd(n,\gamma)^{156}Gd + 8536$ keV (σ_T=61000 b), ^{155}Gd – 14.8% in natur. Gd
$^{157}Gd(n,\gamma)^{158}Gd + 7937$ keV (σ_T=254000 b), ^{157}Gd – 15.7% in natur. Gd

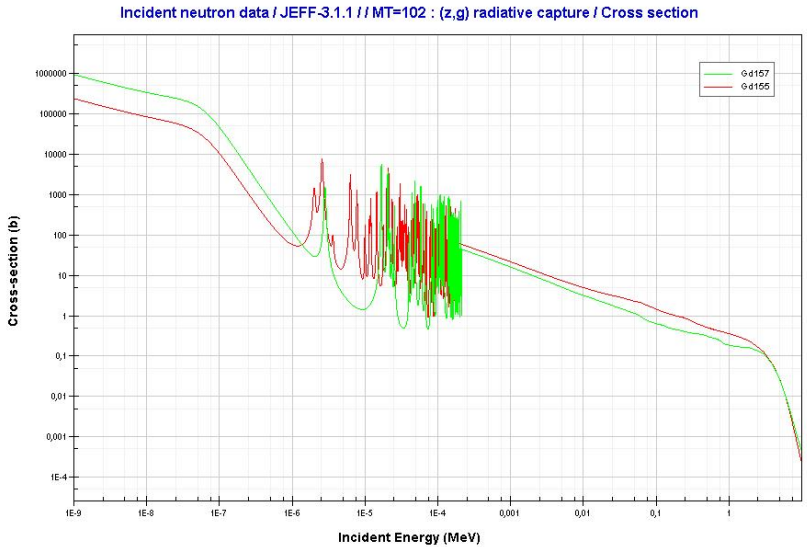

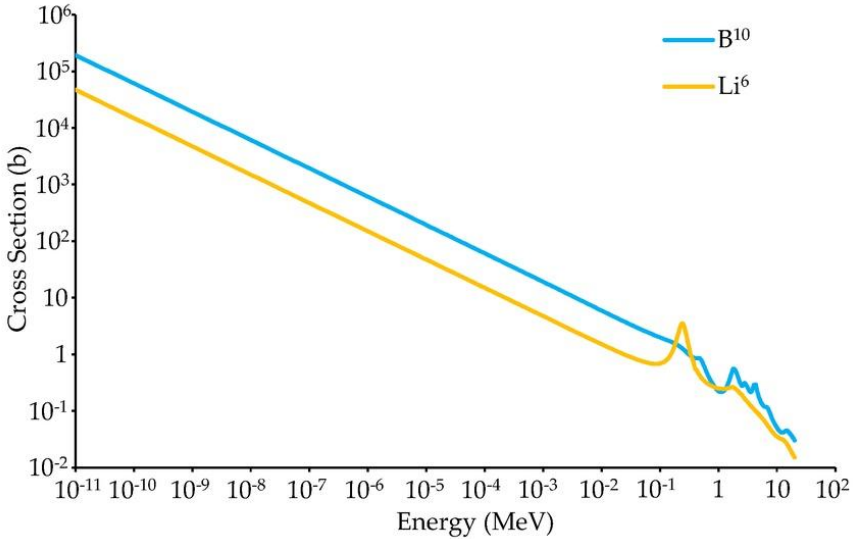

Main reactions for thermal neutrons detection

To register thermal neutrons in scintillation detectors, the following reactions are most often used:

^{6}Li(n,α)t (^{6}LiI:Eu, Cs_2LiYCl_6:Ce (CLYC), $Cs_2LiLaCl_6$:Ce (CLLC), Cs_2LiYBr_6:Ce (CLYB)…)

^{155}Gd(n,γ)^{156}Gd, ^{157}Gd(n,γ)^{158}Gd (GAGG:Ce, GSO, GOS, GdI_3:Ce…)

Li-containing scintillators:

+ Low sensitivity to background gamma radiation;
+ Short range of reaction products in the scintillator material;

-Low light yield;
-Rapid drop in reaction cross-section with increasing neutron energy;
-Need for enrichment in the ^{6}Li isotope;

Gd-containing scintillators:

+ No need for isotope enrichment;
+ New reaction channels appear with increasing incident neutron energy;
+ High light yield;

- Large mean free path of reaction products in the substance;

Scintillation materials based on rare earth elements for neutron registration

Chemical formula	Light yield, ph/MeV	Decay time, ns	Density, g/cm³	Z_{eff}	Thermal capture cross section, b
$Lu_3Al_5O_{12}$:Ce (LuAG:Ce)	24000	55-65	6,67	62,9	77 (Lu)
$Gd_3Al_2Ga_3O_{12}$:Ce (GAGG:Ce)	~58000	90-170	6,2	54,4	49000 (Gd) / 2,9 (Ga)
Lu_2SiO_5:Ce (LSO:Ce)	~30000	40	7,4	66,4	77 (Lu)
Gd_2SiO_5:Ce (GSO:Ce)	12500	56;600	6,71	59,4	49000 (Gd)
$Lu_{2(1-x)}Y_{2x}SiO_5$:Ce (LYSO:Ce)	32000	30-35	7,2	63-65	77 (Lu) / 1,0 (Y)
$GdBr_3$:Ce	44000	20 (26%), 212 (65%), 13500 (9%)	4,55	52,4	49000 (Gd) / 6,8 (Br)

Neutron interaction cross section

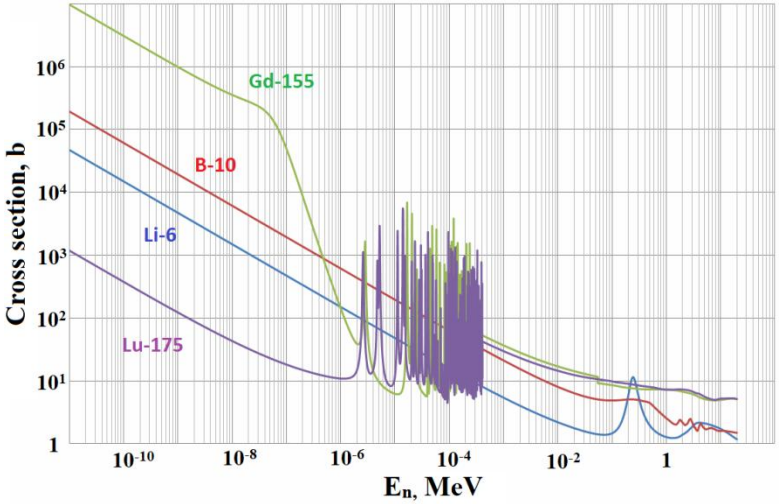

$GdBr_3$

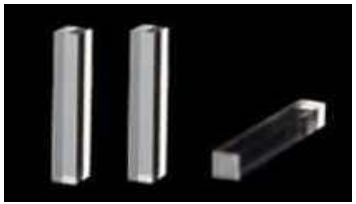

LYSO

GAGG

The best way – $Ga_3Al_2Ga_3O_{12}$ (GAGG):
- high light yield
- non-hygroscopic
- without natural radioactivity

GAGG:Ce (n,γ) multiplicity

$^{155}_{64}Gd + {}^{1}_{0}n \rightarrow {}^{156}_{64}Gd + \gamma$ 8,5358 МэВ

$^{157}_{64}Gd + {}^{1}_{0}n \rightarrow {}^{158}_{64}Gd + \gamma$ 7,937 МэВ

During photonuclear reactions (n,γ) on Gd the cascade of 3-4 gamma quanta (on the average) are emitted – **multiplicity effect**.

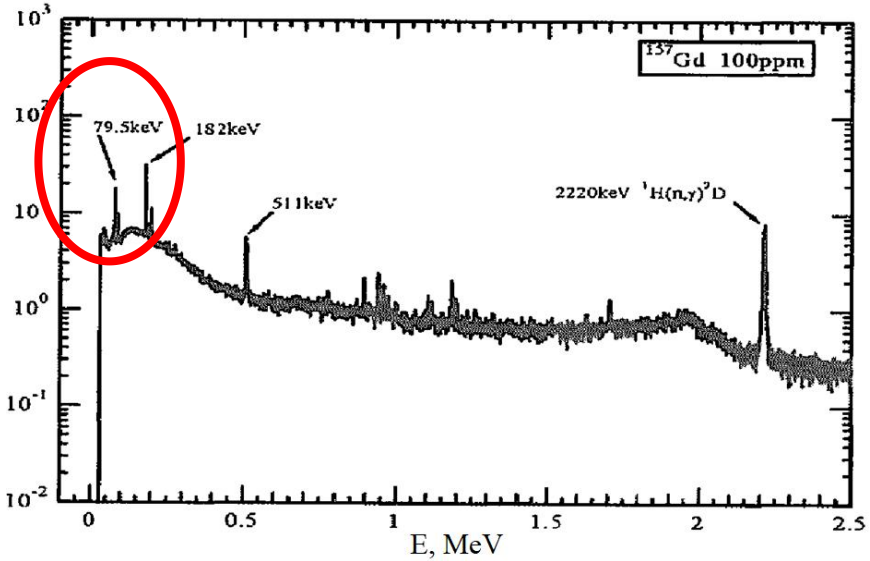

Multiplicity leads to the formation of low-energy lines in the gamma-ray spectrum, along which neutrons can be recorded.

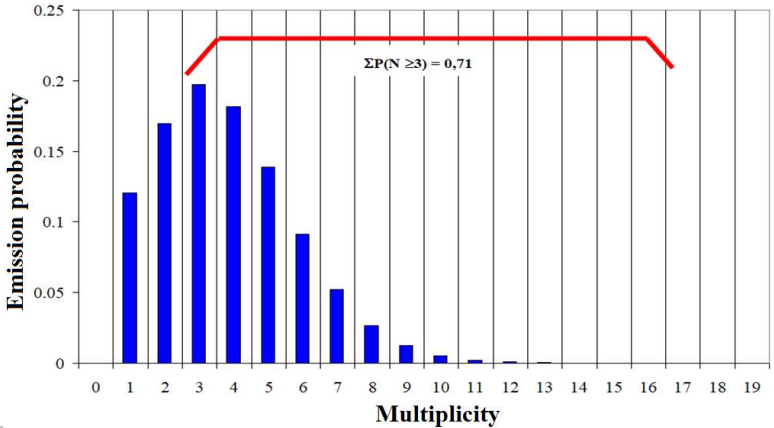

The histogram of the gamma-quanta emission probability for different multiplicity values during the Gd(n,g) reaction.

Gd natural isotopes composition has the thermal neutron's absorption cross-section on the level of **49000 barns** + resonances from 1 eV to 10 keV. This allows Gd-containing scintillators to detect neutrons in an expanded energy.

Moreover, at higher neutron energy, the other reaction channels such as inelastic scattering, (n,p), (n,α), etc. on Al, Ga and O nuclei become open, increasing the stopping power of GAGG to neutrons.

Optimization of crystal scintillation parameters $Gd_3Al_2Ga_3O_{12}$:Ce (GAGG:Ce)

The main parameters of the scintillation material that determine the properties of the detector: **light yield** (LY), **rise time** (τ_r), **decay time** (τ_d).

When neutrons are registered with a gadolinium-containing scintillator, mainly low-energy gamma quanta are emitted, therefore, increased requirements are imposed on both the scintillation yield LY and the kinetics of the scintillation pulse, especially τ_r

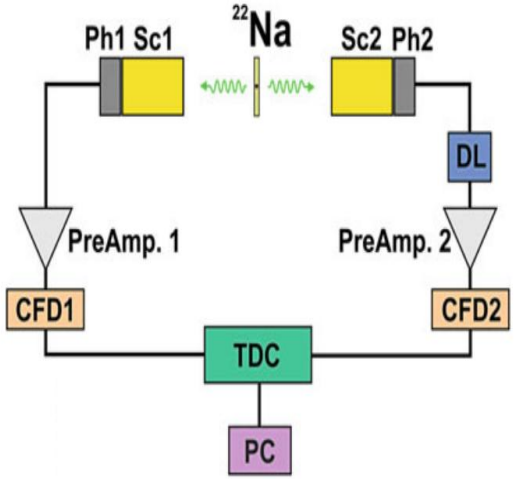

Energy resolution ~ $1/(LY)^{1/2}$
Time resolution ~ $(\tau_r \cdot \tau_d/LY)^{1/2}$

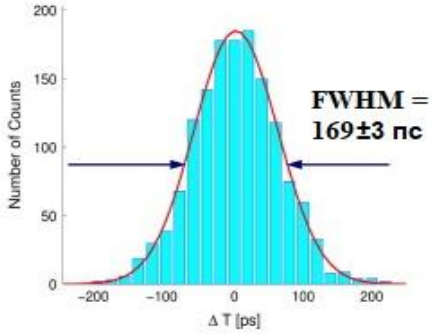

GAGG parameters before optimization:

Decay time τ_d, ns	Time resolution in coincidence mode (CTR, +20 °C), ns	Energy resolution @ γ 511 keV, %	LY, photons/MeV	emission spectrum max., nm	Phosphorescence
89 (73%)	**1.39**	8.0	~50000	525	+

GAGG radiation resistance and optimization

GAGG parameters **after** optimization:

After optimization of doping with Mg, the GAGG:Ce,Mg showed high radiation resistance to gamma and proton irradiation.

Decay time τ_d, ns	**33 (30%), 86 (56%), 130 (14%)**
CTR (+20 °C), ns	**0.165 ± 0.03**
Energy resolution @ γ 511 keV, %	**7,6**
LY, photons/MeV	**39000**
Emission spectrum max., nm	**540**

GAGG:Ce time resolution (CTR) vs energy

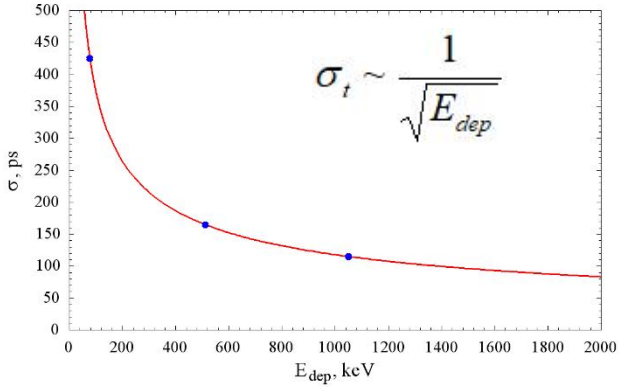

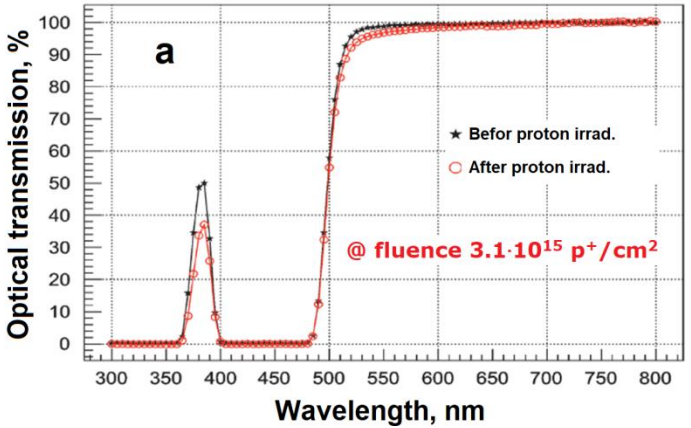

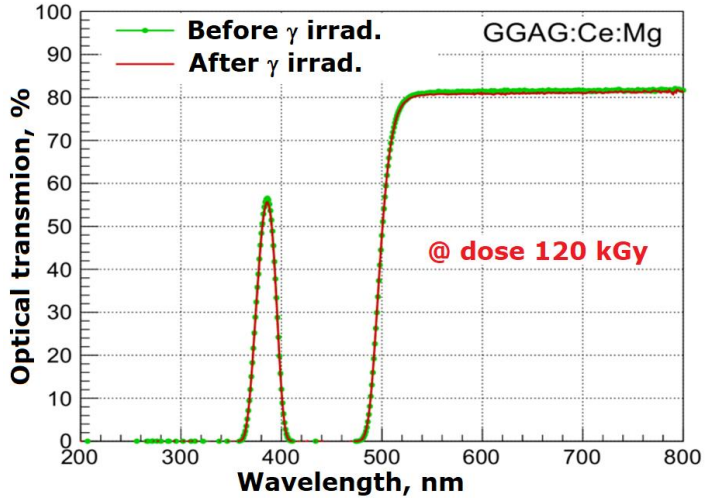

Mg co-doping:

- reduces rise time of scintillation
- suppression of the slow decay time component
- improving time resolution (CTR)
- elimination of phosphorescence

The achieved parameters of the material made it possible to start creating neutron detectors based on it.

GAGG:Ce response to neutrons

ATOMTEX®

Neutron AT140 bench

^{241}Am-Be response:

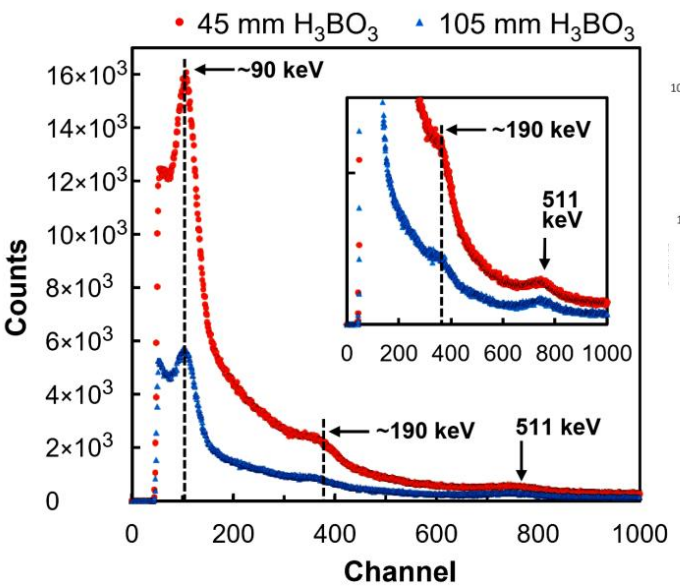

Compact and Effective Detector of the Fast Neutrons on a Base of Ce-doped Gd3Al2Ga3O12 Scintillation Crystal / M. Korjik [et al.] //IEEE TNS. - 2019. - Vol. 66. - PP.536-540.

^{238}Pu-Be response:

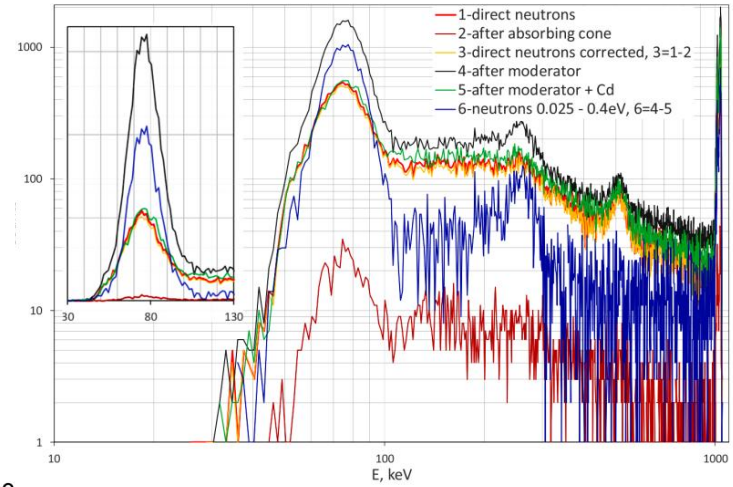

Sensitivity of GAGG based scintillation neutron detector with SiPM readout / A. Fedorov [et al.] // Nucl. Engin. and Techn. - 2020. - Vol. 52. - PP.2306-2312

Carry out studies with GAGG samples at Pu-Be and Am-Be neutron sources (E_n up to 10-12 MeV) have shown that:

GAGG 14×14×10 mm has neutron detection efficiency from 9.29% for fast neutrons till 64.6% for E_n < 0.4 eV – in 45-300 keV gamma quanta energy scale.

GAGG for registration of fast and relativistic neutrons

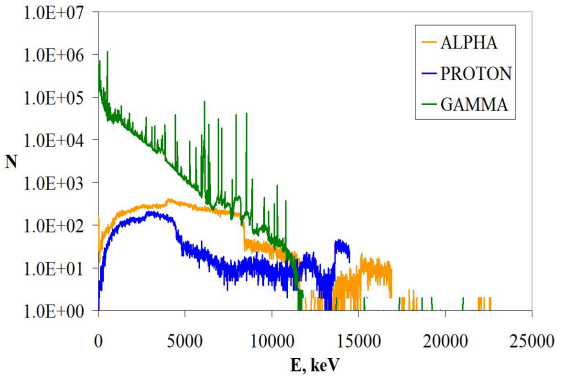

Spectra of particles emitted in GAGG upon capture of 14.6 MeV neutrons (GEANT4 simulation)

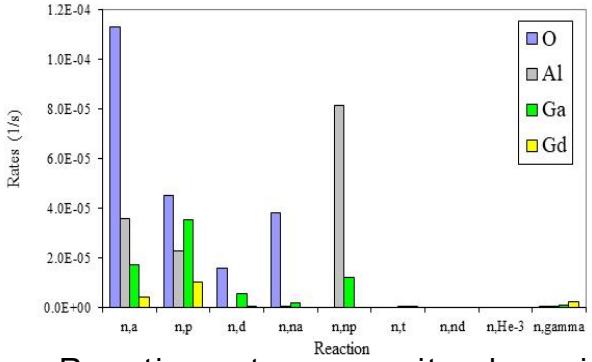

Reaction rates per unit volume in GAGG:Ce

Reaction rate:

$$\frac{dN}{dt} = j \cdot n \cdot S \cdot l \cdot \sigma$$

where **n** is the concentration of target nuclei, **S** - target area, ***l*** - target thickness, **j** - neutron flux density and **σ** - reaction cross-section.

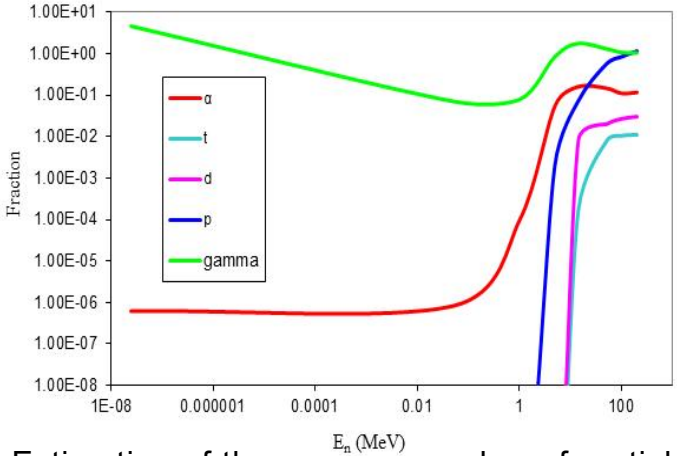

Estimation of the average number of particles of different types emitted upon neutron capture in GAGG:Ce

Signals from secondary protons should dominate the response spectrum of charged particles, while at the same time they should be shifted to the low-energy region relative to α-particles.

The dominant reaction for thermal neutrons is the radiation capture reaction (n,g), which gives way to other channels with increasing neutron energy – after 5-8 MeV, the most significant reactions are those with the emission of protons and alpha particles: (n,a), (n,n+a), (n,p) and (n,n+p)

Scintillation ceramics GYAGG:Ce

Dilution of the Gd sublattice in GAGG will lead to a reduction in the excitation migration distance, which will have a positive effect on reducing the scintillation pulse formation time.

Sample	GAGG:Ce,Mg (reference)	GYAGG:Ce,Mg after the first growth process
Scintillation decay constants, ns, and relative weight, (%)	28 (30) 68 (52) 168 (18)	36 (80) 97 (20)
Average decay constant τ_{sc}, ns	72	48
Light yield, ph/MeV	41000	52000

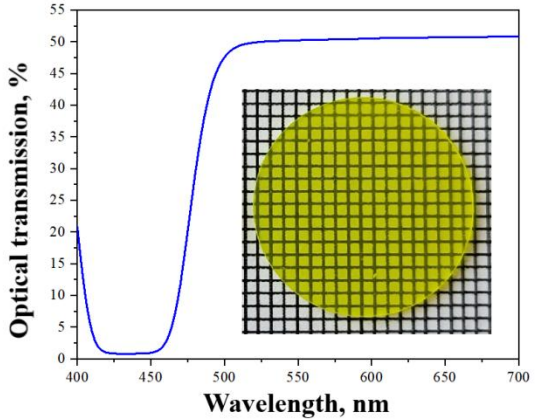

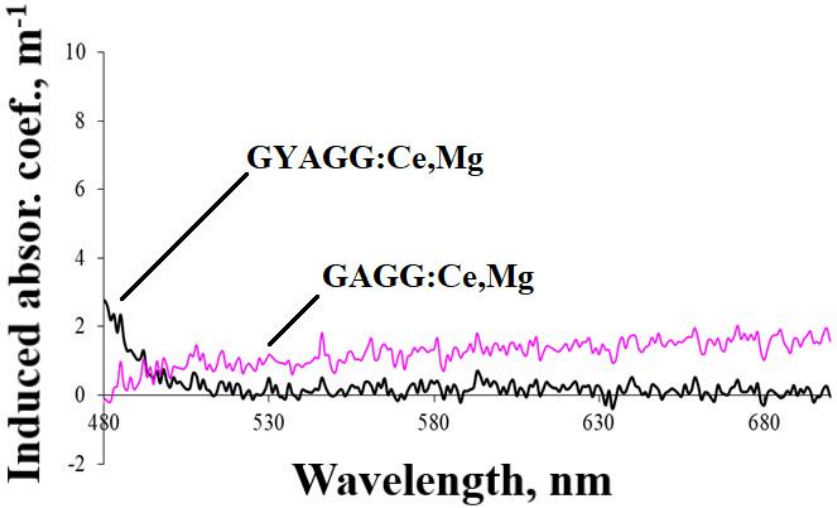

Spectrum of induced optical absorption in the spectral range scintillations of GAGG:Ce,Mg and GYAGG:Ce,Mg after irradiation with a ^{60}Co γ-source up to 2000 Gy.

Scintillation silicate glass with the addition of Ba and Gd

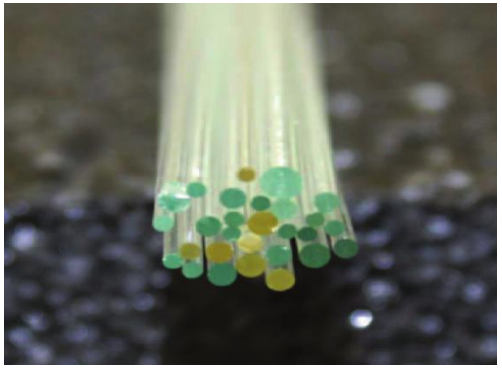

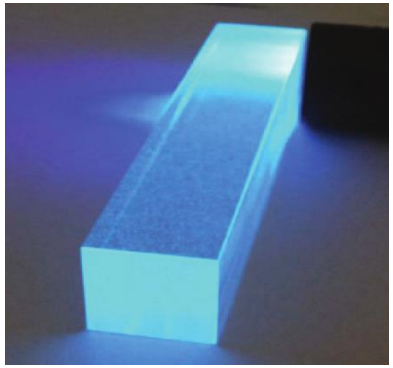

Samples of the developed scintillation material Ba-Gd-Si:Ce

Chemical composition of glass, mol.%	Density, g/cm3	Maximum emission spectrum, nm	Scintillation decay times and their weighting factors, ns	Time resolution (CTR), ps	Light yield, ph/MeV	LY temp. drift, %/°C
SiO_2 – 63 BaO – 22 AlF_3 – 1,4 Ce_2O_3 – 0,76 Gd_2O_3 – 13,09	4,2	410	90 (45%) 400 (55%)	230 ± 65	2500	0,3

Scintillation silicate glass with the addition of Ba and Gd

New glass Gd-Al-Si:Ce:

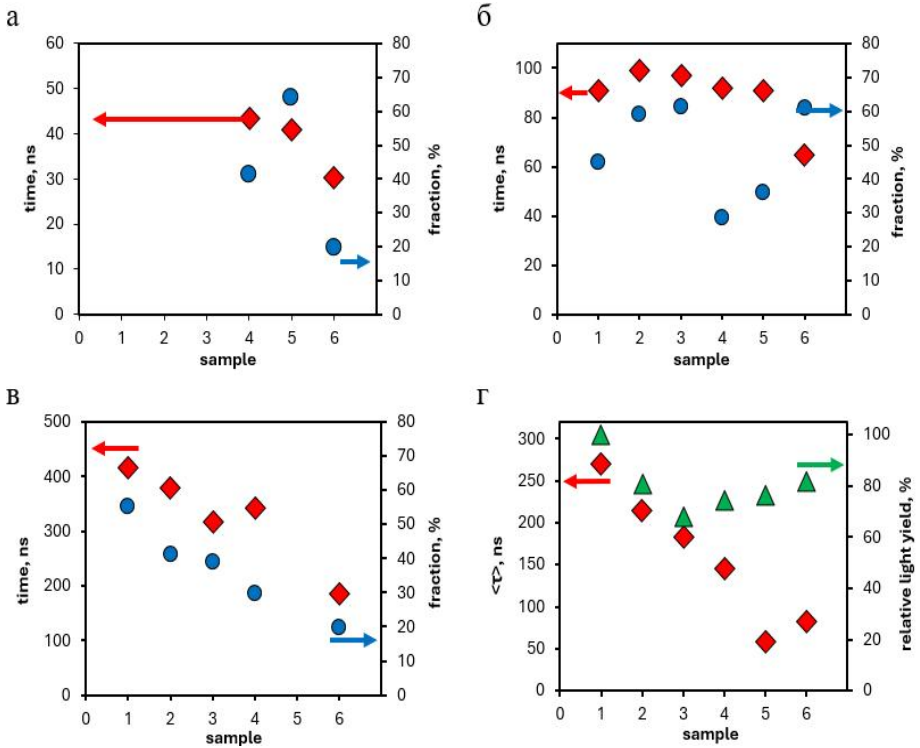

Changes in the components of scintillation emission kinetics and their proportions (a-c), as well as the average decay time and light output (g) of the samples.

[Journal of Non-Crystalline Solids. – 2022. – Vol. 580. – PP. 121393]

Glass	Ba-Gd-Si:Ce (comparison sample)	Gd-Al-Si:Ce
Scintillation decay times and their weighting factors, ns	90 (45%) 400 (55%)	93 (62%) 317 (38%)

- A new scintillation glass Gd_2O_3-Al_2O_3-SiO_2 doped with Ce^{3+} ions has been developed. The glass demonstrated scintillation decay kinetics with an average decay time of 60 ns and a light yield of ~2000 photons/MeV. The glass density is 4.7 g/cm^3.
- The scintillation decay kinetics in Gd-Al-Si glass are significantly faster than in Ba-Gd-Si glass, while the light yield is reduced relatively insignificantly (~15%).

Prototype of calorimetric cell based on Ba-Gd-Si:Ce glass for NICA (JINR)

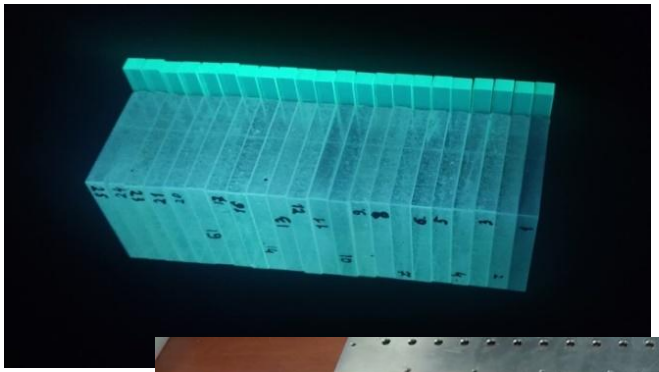

Scintillation silicate glass with the addition of Li

$$^{6}_{3}Li + n_{therm} \rightarrow {}^{3}_{1}H(E_t = 2.73\ MeV) + {}^{4}_{2}He(E_\alpha = 2.05\ MeV)$$

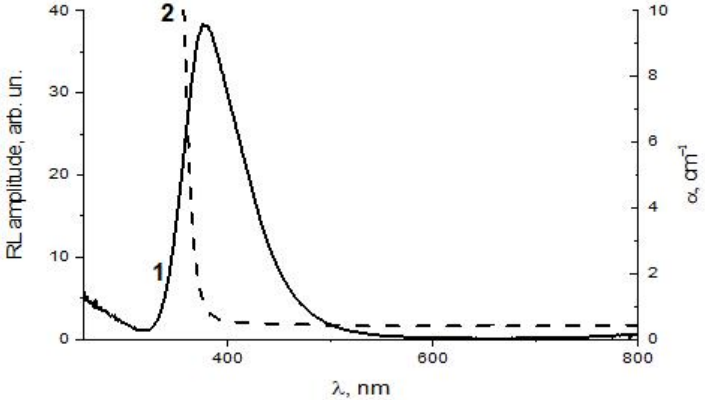

Radioluminescence spectrum of $Li_2O{\cdot}2SiO_2$:Ce (DSL) glass (1) and absorption (2).

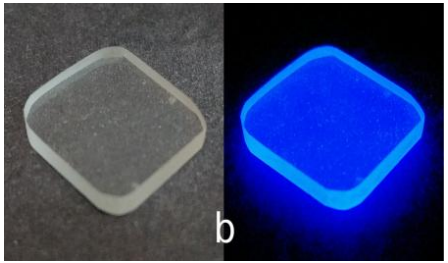

UV phosphorescence (312 nm) of DSL glass

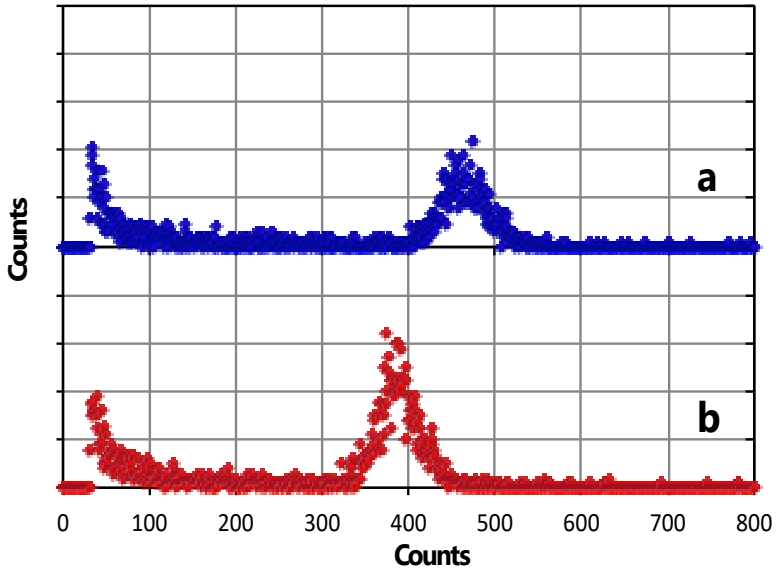

Response to a thermal neutron source (^{252}Cf+30 cm graphite) with glass DSL (20x20x7 mm) (a) and glass GS20 (Ø10×7 mm) (b).

DSL glass response to thermal neurons: 15% greater than for GS20.

Lightweight polycrystalline scintillator Li_2CaSiO_4:Eu – LCS

The search for light scintillation materials for neutron detection with increased scintillation yield was relevant.

Li_2CaSiO_4:Eu (LCS) exhibits high scintillation properties and is promising for the creation of neutron-sensitive screens based on it. Light yield ~12000 ph/MeV.

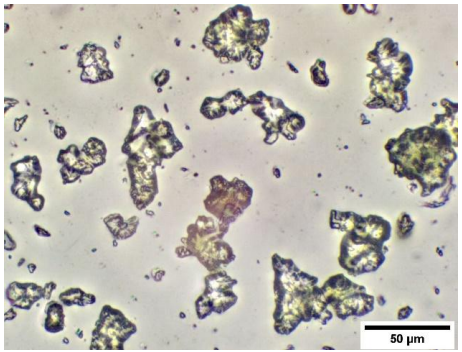

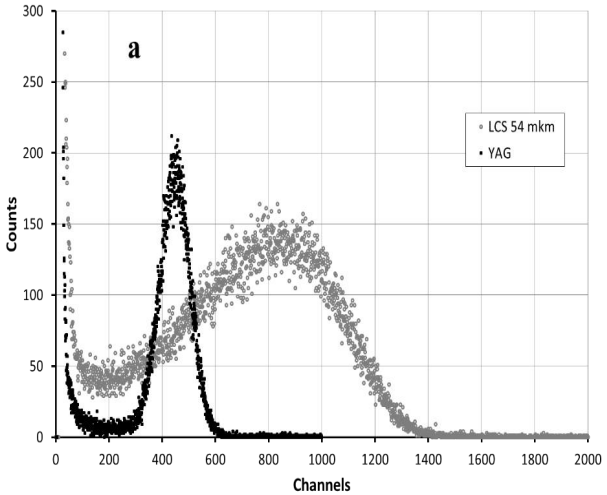

α-particle spectrum for a 54 µm thick LCS sample compared to a YAG:Ce reference scintillator.

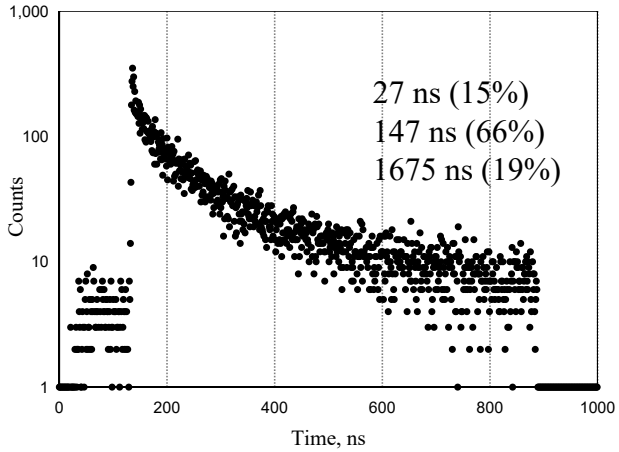

Scintillation kinetics of $^6Li_2CaSiO_4$

[Nul. Instrum. and Meth. in Phys. Res. A. – 2023. – Vol. 1045. – PP.167637.]

Thermal neutron detection: event selection methods.

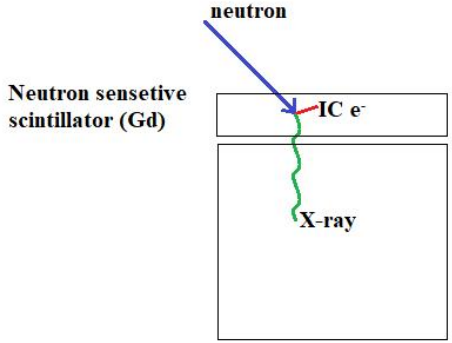

When neutrons interact **with Gd nuclei**:

- Conversion electrons (IC) and characteristic X-ray radiation are emitted.
- The electrons are completely absorbed in the neutron sensitive sample.
- The characteristic X-ray radiation is absorbed in the neutron non-sensitive sample.

Coincidence method can be implemented.

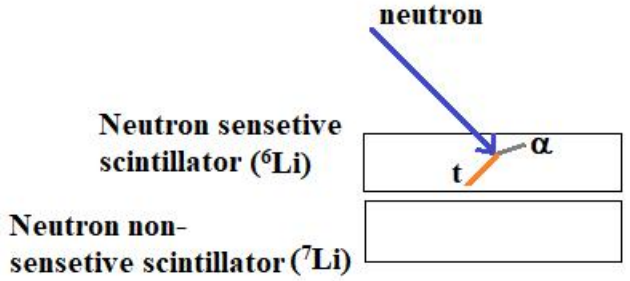

When neutrons interact **with Li nuclei:**

- The reaction products are completely absorbed in the thickness of the neutron-sensitive sample
- The background gamma radiation interacts with both neutron sensitive and neutron non-sensitive samples.

Anticoincidence method can be implemented.

Thermal neutron detection: 2CH detector with COINC/ANTI-COINC mode

The main requirements for a neutron detector:

1. High selectivity to neutrons.
2. Low sensitivity to gamma quanta.

The prototype uses two sets of samples: **GYAGG + YAGG** scintillation ceramics and **^{6}DSL + ^{7}DSL** lithium glasses.

Sample	Chemical composition	Dimensions, mm^3	Light yield, ph/MeV	Kinetics τ, ns
GYAGG	$^{nat}Gd_{1,5}Y_{1,5}Al_{2.5}Ga_{2.5}O_{12}$:Ce, Mg	14.6×14.6×**0.23**	41000	21 (31%) 60 (48%) 646 (21%)
YAGG	$Y_3Al_{2.5}Ga_{2.5}O_{12}$:Ce,Mg	14.6×14.6×**1.25**	43000	33 (56%) 61 (44%)
^{6}DSL	$^{6}Li_2O$*2SiO_2:Ce	12.0×15.0×**0.50**	6000*	42 (48%) 96 (33%) 600 (19%)
^{7}DSL	$^{7}Li_2O$*2SiO_2:Ce	12.0×15.0×**0.50**	6000*	42 (48%) 96 (33%) 600 (19%)

* - ph/neutron

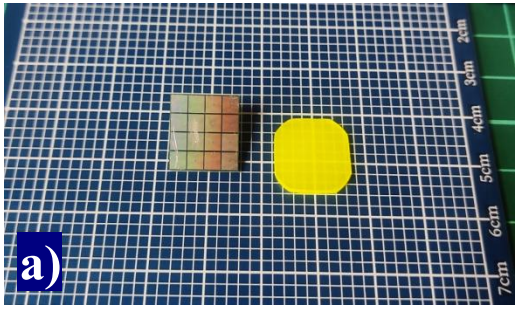

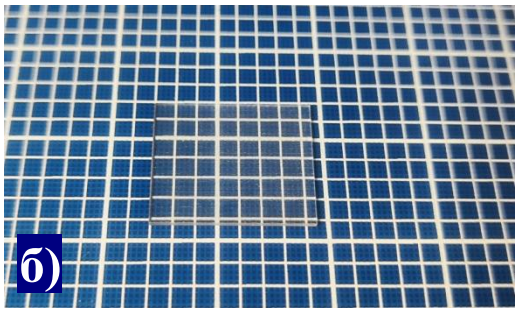

GYAGG (a) и ^{6}DSL (b)

Thermal neutron detection: 2CH detector with COINC/ANTI-COINC mode

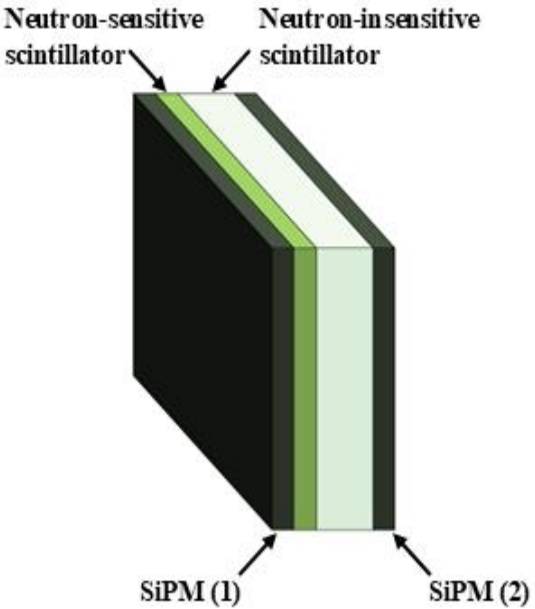

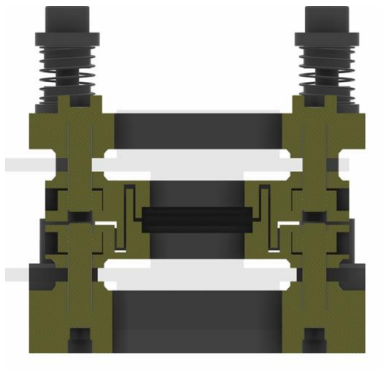

A 188 μm Lumirror reflector is placed between the DSL glasses, and a 9 μm Al layer is placed between the ceramic samples.

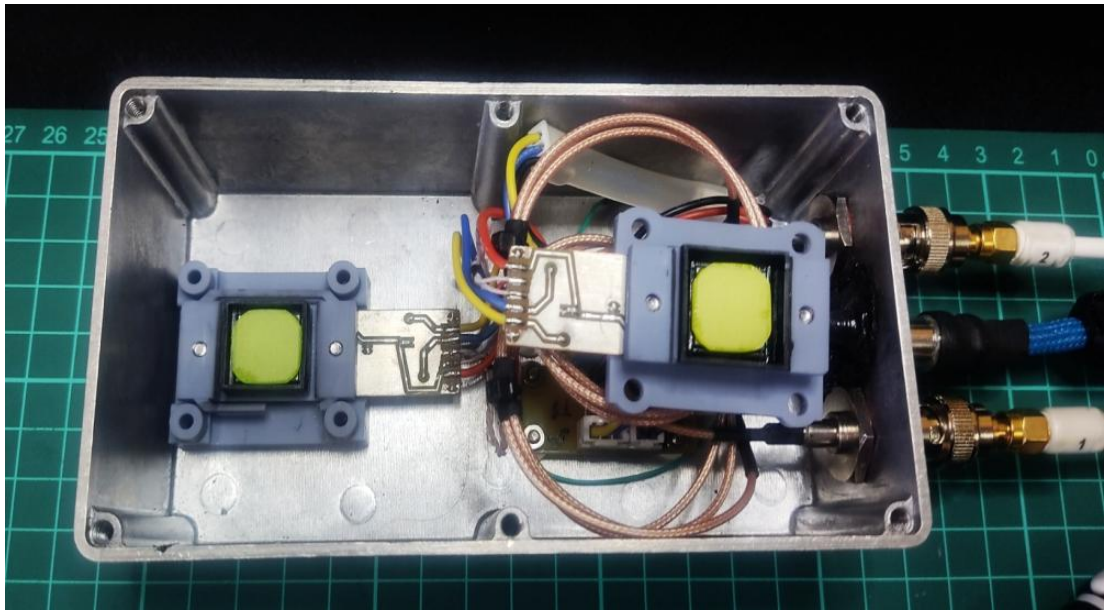

Thermal neutron detection: 2CH detector with COINC/ANTI-COINC mode

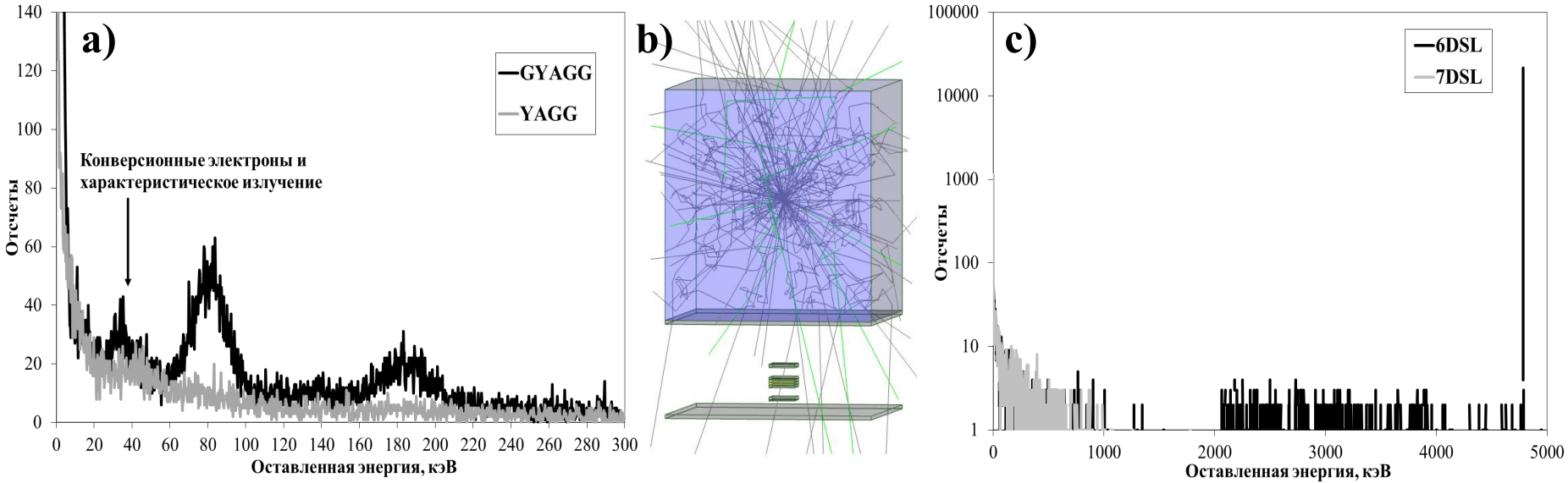

Simulation of the response of scintillation ceramics (a) and lithium glasses (b) to thermal neutrons and visualization of the simulated geometry (c)

In the model spectra of scintillation ceramics: a peak of coincidence of conversion electrons and characteristic radiation absorption events is observed.

In the model spectra of Li-glasses: there is no absorption of reaction products in a neutron-insensitive sample.

Thermal neutron detection: 2CH detector with COINC mode

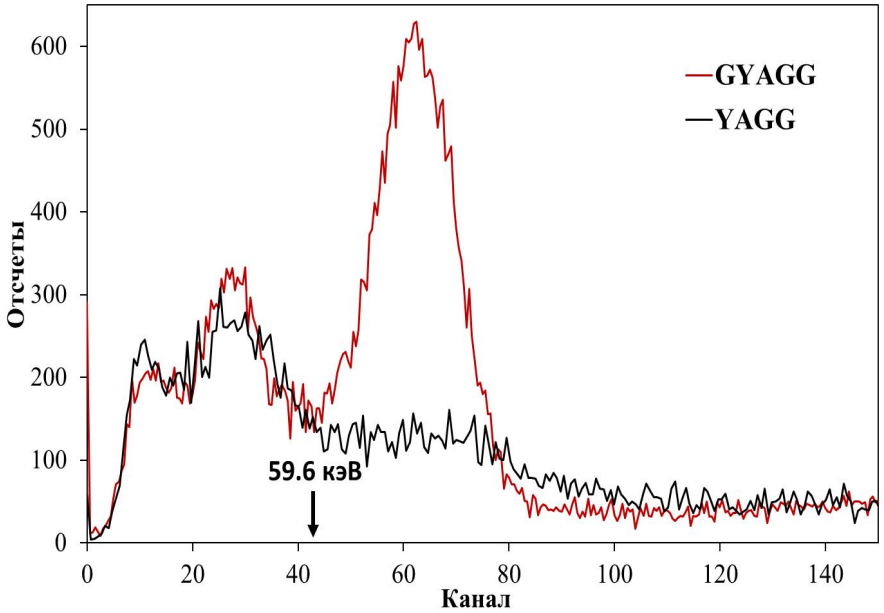

Thermalized neutron response spectrum

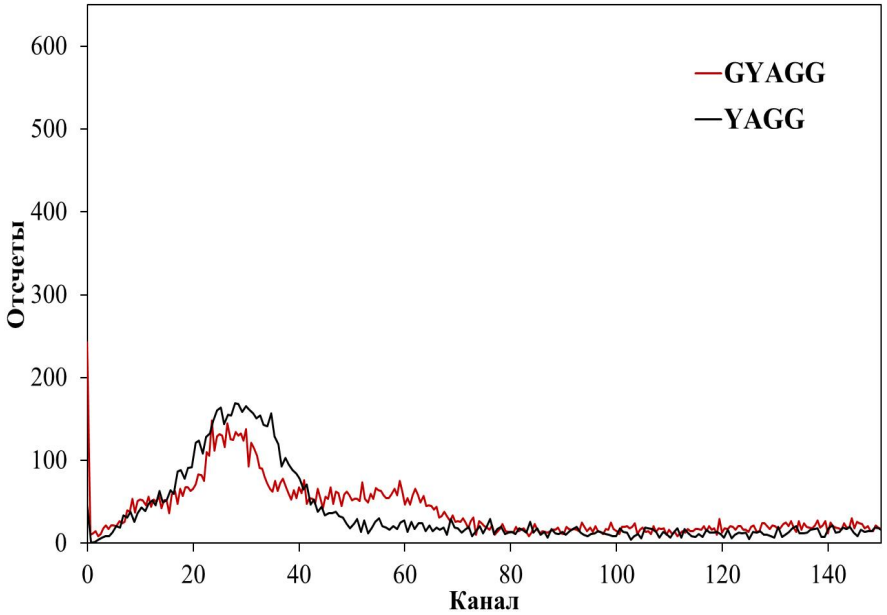

Response spectrum in coincidence mode

The efficiency of thermal neutron registration by the GYAGG sample is 19%, in the coincidence mode – 4.1% for GYAGG, 5.2% for YAGG. The efficiency of neutron registration in the coincidence mode decreases by 3.65 times, gamma quanta – **by 10 times.**

Thermal neutron detection: 2CH detector with ANTI-COINC mode

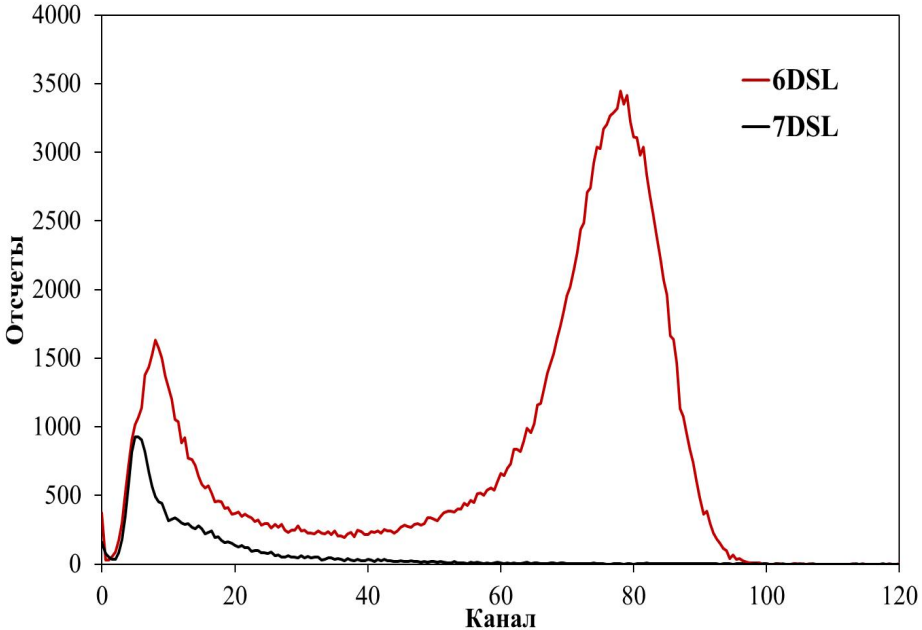

Thermalized neutron response spectrum

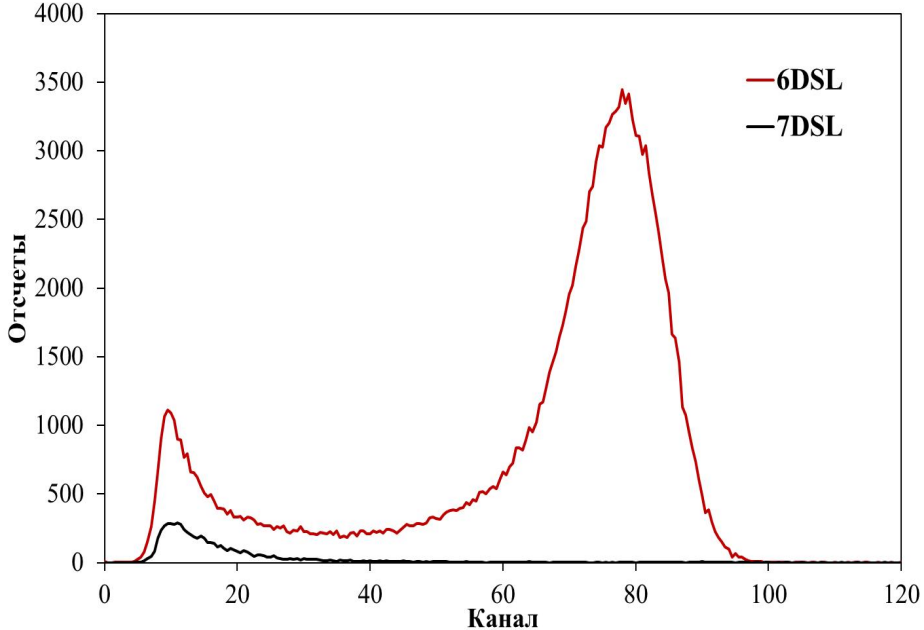

Response spectrum in coincidence mode

The efficiency of thermal neutron detection by the 6DSL sample is 69.2%. In the anticoincidence mode, the efficiency of background gamma radiation detection decreases by a factor of 2.25.

Thermal neutron detection: 16CH detector

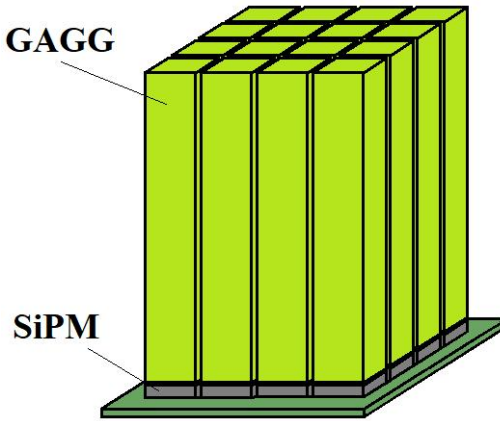

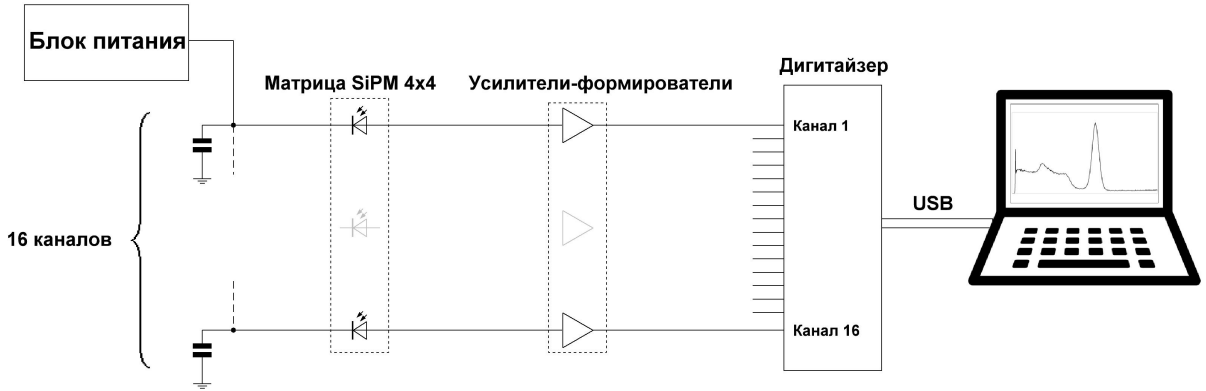

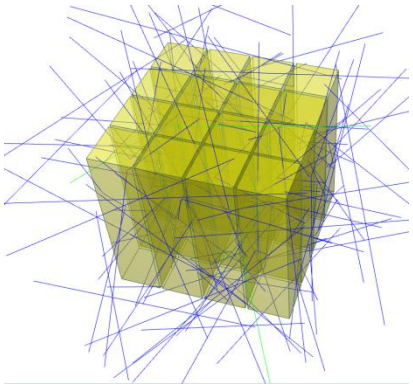

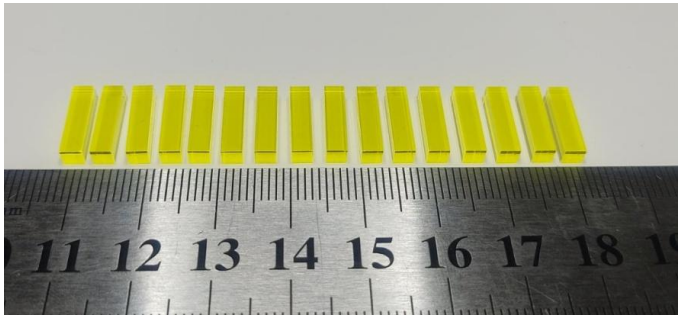

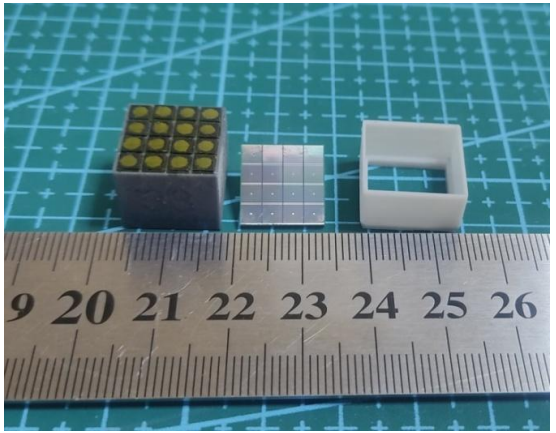

Thermal neutron detection: 16CH detector

Multi-hit events registration

Under gamma (661 keV)

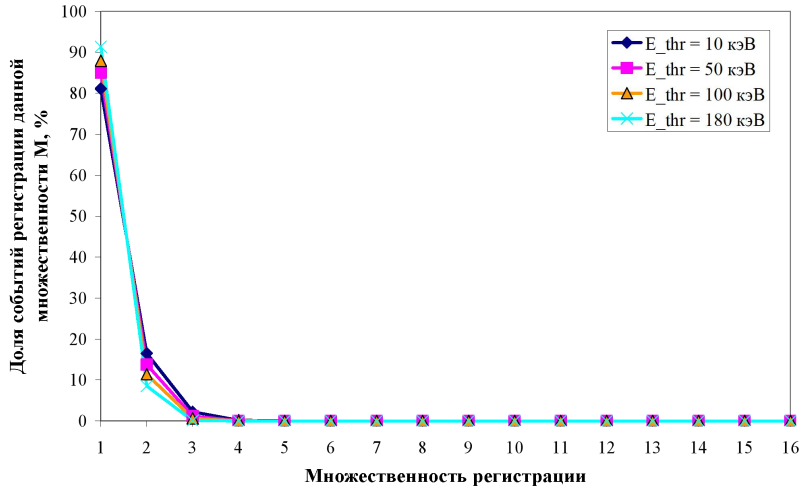

Under neutons (thermal, Pu-Be and 14,6 MeV)

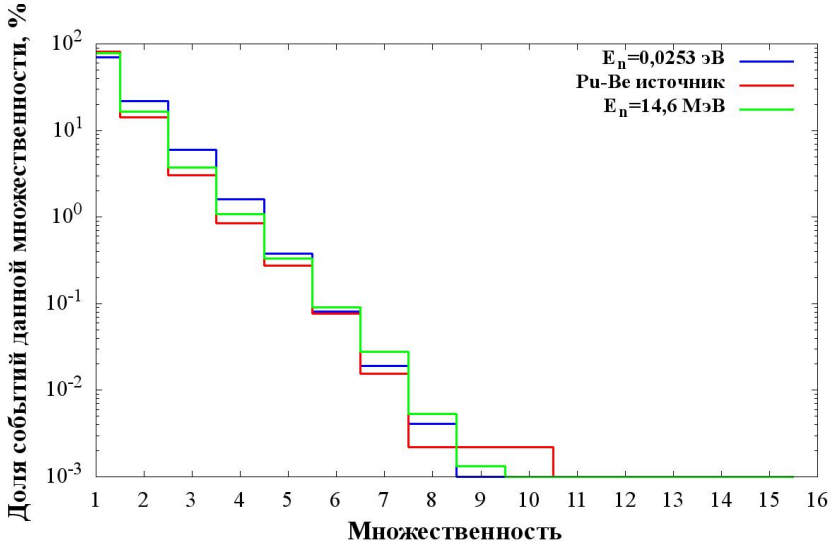

Thermal neutron detection: 16CH detector

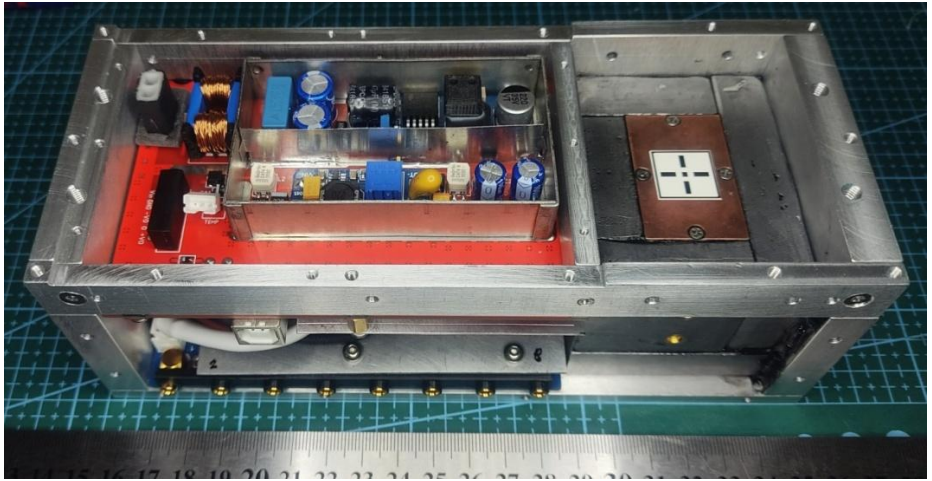

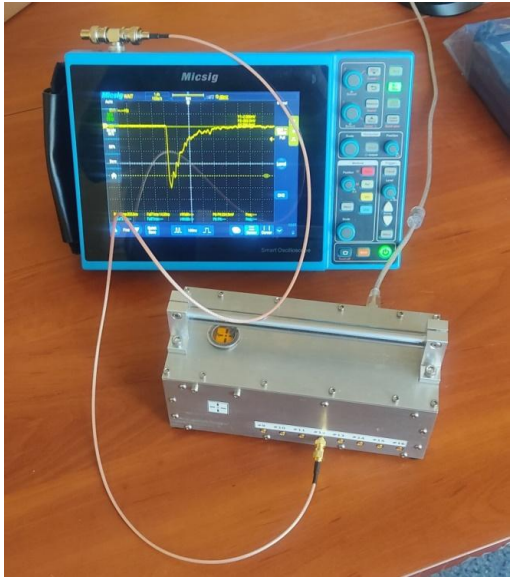

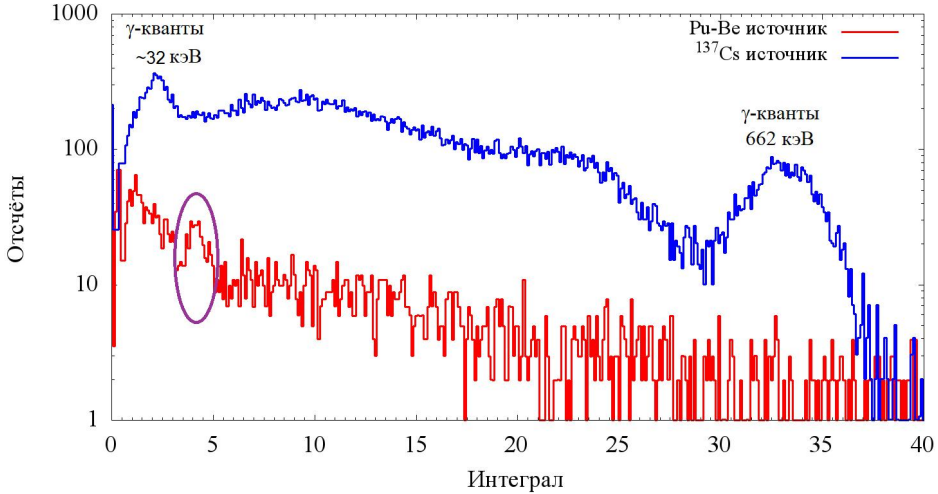

Pulse shape discrimination (PSD) method

The scintillation decay rate can be described by two components: fast (~10-50 ns), and slow (~100-1000 ns). The contribution of the slow component to the total emission intensity may depend on the type of ionizing particle.

The contribution of the slow component depends on the specific ionization energy loss dE/dx of the particle: the larger dE/dx, the larger the contribution of the slow component.

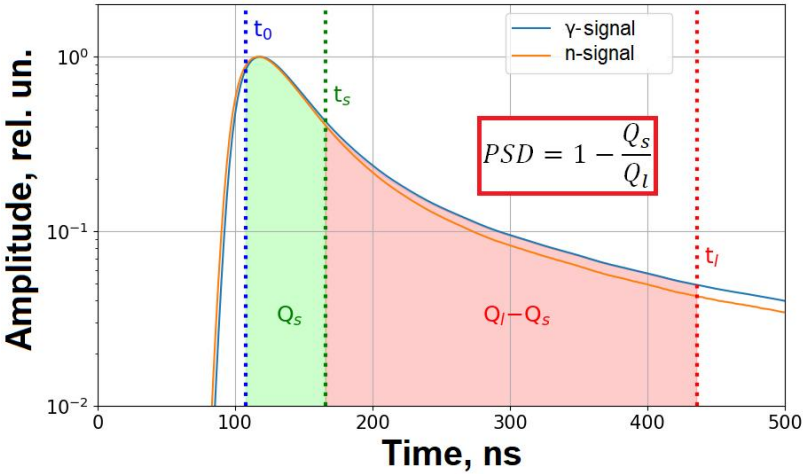

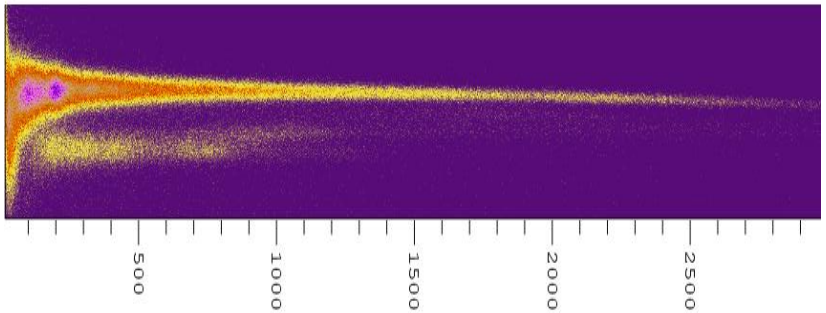

GAGG PSD spectrum @ E_n=14.6 MeV irrad.

This effect can be used to identify the type of particle using pulse shape discrimination method.

GAGG for registration of fast and relativistic neutrons: experiments

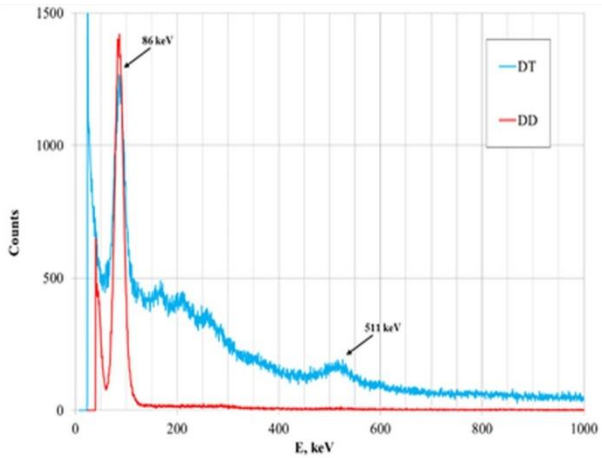

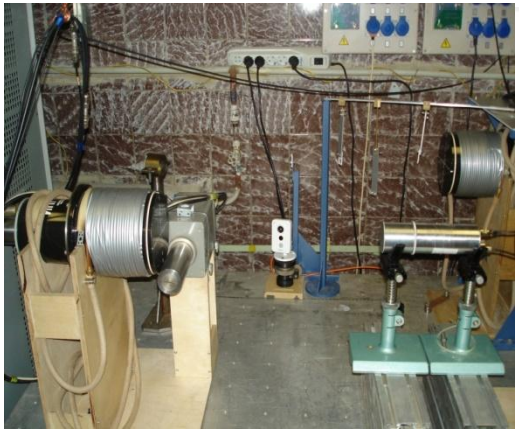

Response of GAGG:Ce to Neutron Radiation from DT- and DD-generators

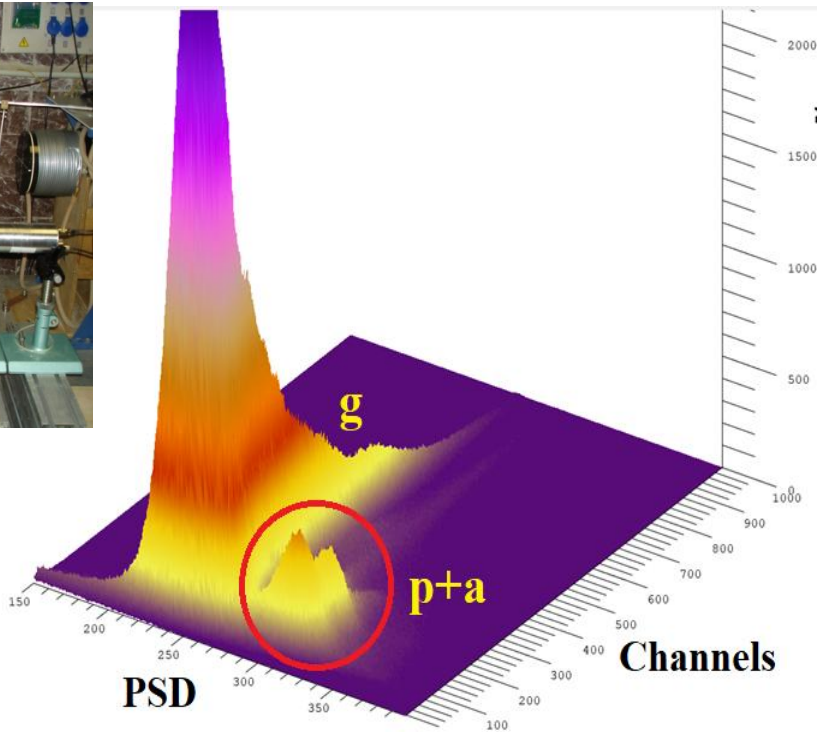

Three-dimensional histogram of GAGG:Ce crystal pulses recorded during irradiation with 14.6 MeV neutrons

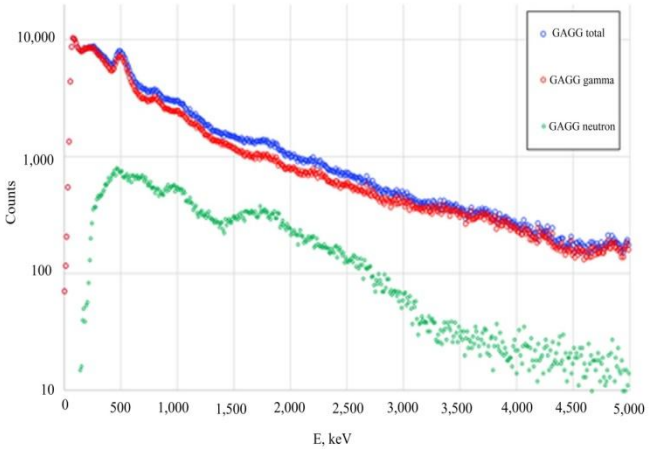

Separation of signals caused by fast neutrons and γ-quanta

Композитный сцинтилляционный экран типа «фосвич» на базе LGS

«Фосвич» (phoswich, “**phos**phor sand**wich**”) – комбинация двух сцинтилляторов с разной кинетикой сцинтилляций, подсоединённые к единому фотоприёмнику.

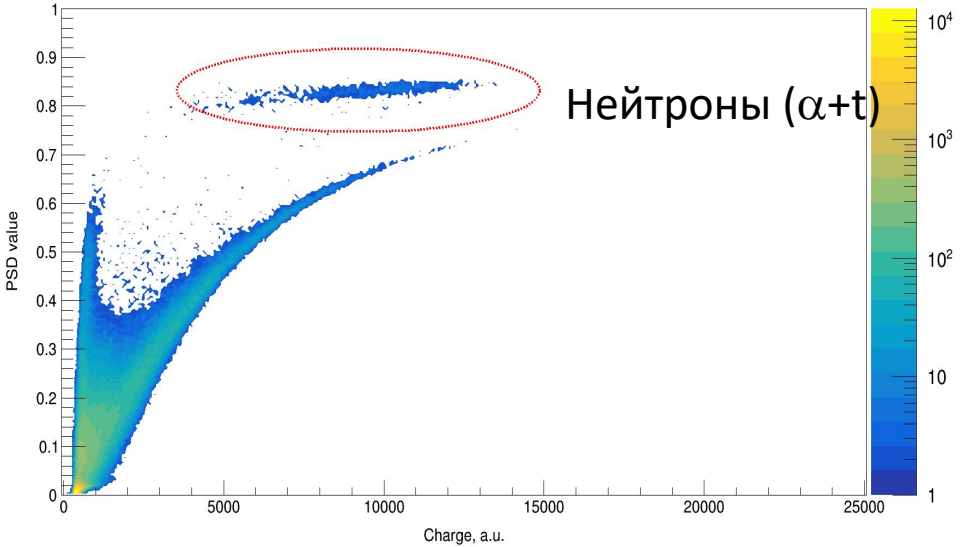

Спектрограмма с разделением сигналов по форме импульсов при регистрации излучения источника ^{252}Cf. Выделена область событий, соответствующая реакции захвата нейтрона ядрами ^{6}Li в слое композита

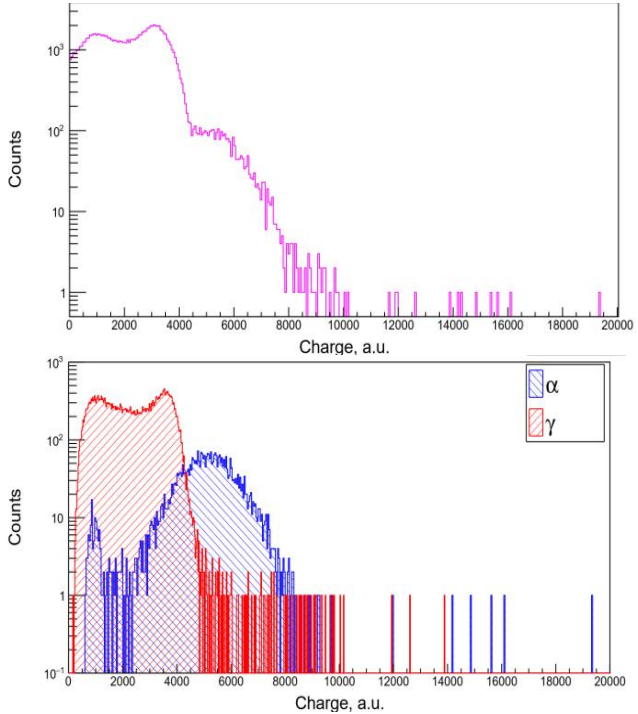

Спектр при одновременной регистрацией альфа-частиц и гамма-квантов фосвичем (а) и разделение спектров площадей под сигналами на основе фильтрации по значению параметра по дискриминации импульсов по форме (PSD).

ToF method

The Time-of-Flight (ToF) method is widely used for spectroscopy of pulsed neutron beams in the energy range from thermal to ~1 GeV.

Basic idea: measure time difference τ from neutrons signal between two detectors (**START** and **STOP**). Neutrons with different energies E_n pass the fixed base L for different time τ.

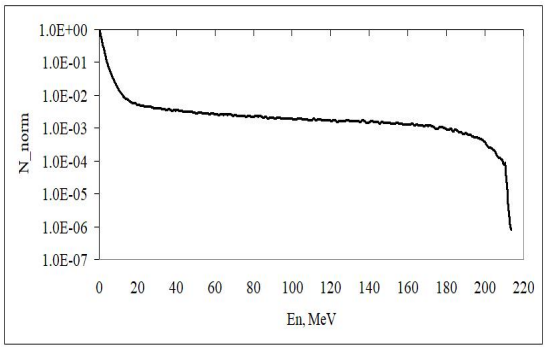

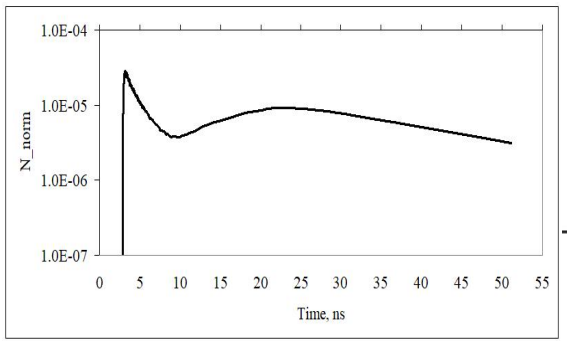

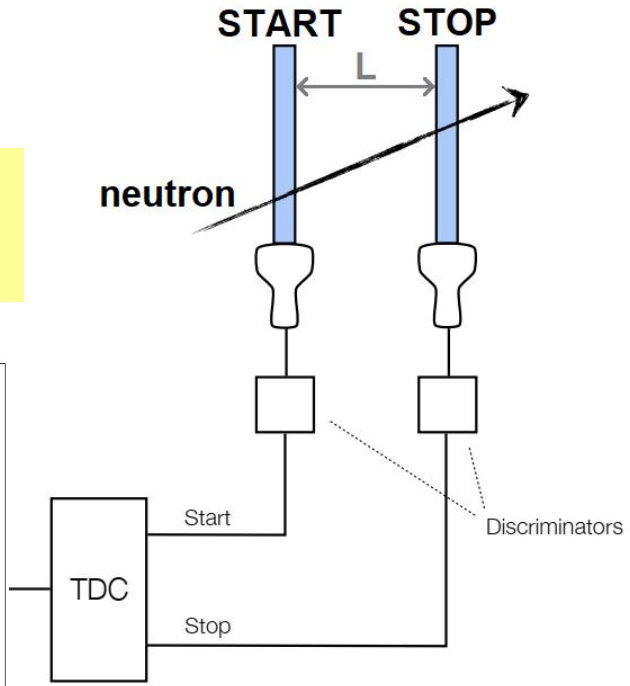

Signals from fast detectors (STAR and STOP) are directed to discriminators that generate pulses for a time-to-amplitude (TAC) or time-to-digital (TDC) converter, the output signal amplitude of which is directly proportional to the time delay τ. **The resulting time spectrum $\varphi(t)$ must be converted into an energy spectrum $F(E_n)$.**

ToF method: transition from non-relativistic to relativistic case

non-relativistic

Neutron kinetic energy:

$$E_n = \frac{mv^2}{2} = \frac{mL^2}{2\tau^2}$$

Spectra converting:

$$F(E) = \frac{1}{m}\frac{\tau^3}{L^2}\varphi(t)$$

Energy resolution:

$$\frac{\Delta E}{E} = \sqrt{\frac{8}{m}}\frac{\sqrt{E}}{L}\Delta t$$

relativistic

$$E_n = mc^2\left(\frac{1}{\sqrt{1-\frac{1}{c^2}\left(\frac{L}{\tau}\right)^2}} - 1\right)$$

$$F(E) = \varphi(t)\frac{1}{m}\frac{\tau^3}{L^2}\left[1-\left(\frac{L}{c\tau}\right)^2\right]^{\frac{3}{2}}$$

$$\frac{\Delta E}{E} = \frac{mc^3}{E_n L}\left(\left(\frac{E_n}{mc^2}\right)^2 + 2\frac{E_n}{mc^2}\right)^{\frac{3}{2}}\Delta t = \frac{c}{L}\sqrt{\gamma}\left(\gamma+2\right)^{\frac{3}{2}}\Delta t$$

m – neutron mass
E_n – neutron kinetic energy
c – velocity of light
v – neutron velocity
L – ToF base
Δt – time resolution
ΔE – energy resolution
τ – ToF value
$\varphi(t)$ – ToF spectrum
F(E) – energy spectrum
γ – relativistic Lorentz-factor

$$\frac{\Delta E}{E} \propto \sqrt{\left(\frac{\Delta t}{\tau}\right)^2 + \left(\frac{\Delta L}{L}\right)^2}$$

$\Delta E/E$ varies as ~ E^2 at high energies, and as $E^{1/2}$ for nonrelativistic neutrons. This feature limits the application of the ToF method for fast neutrons at facilities with small bases L at low time resolution Δt.

ToF method: transition from non-relativistic to relativistic case

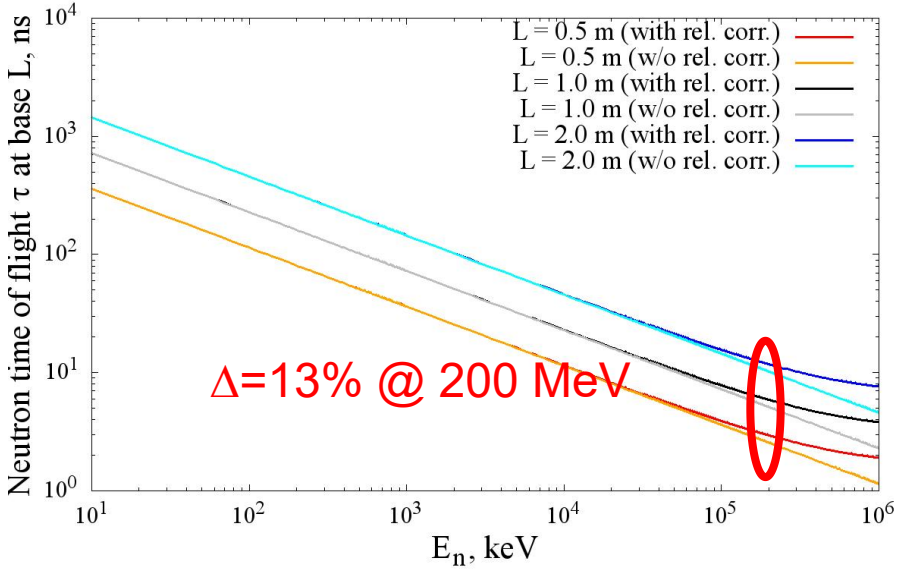

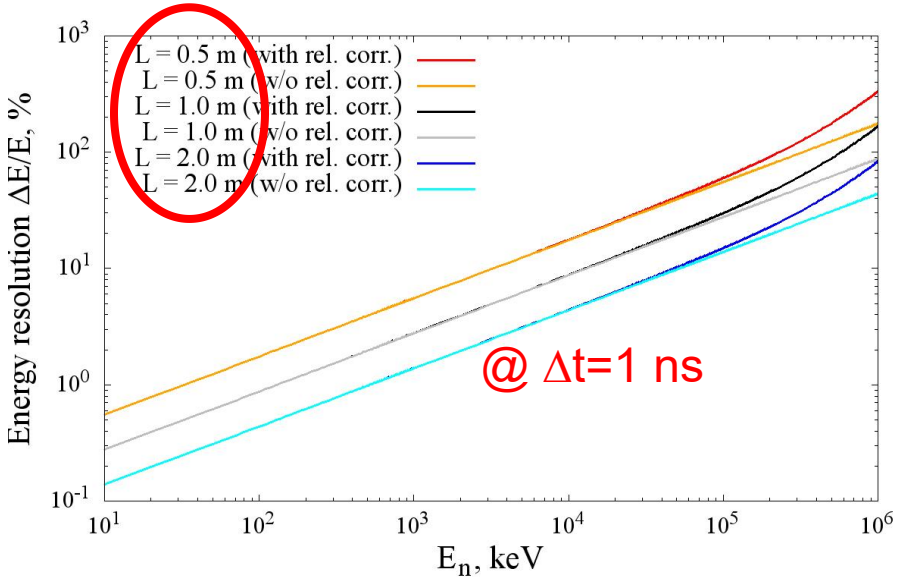

Name	Location	Base L, m	Start/Stop detectors	Energy resolution, %
n-TOF	CERN	185	C_6D_6 + BaF_2	0.11 (20 MeV)
GELINA	Belgium	10-400	C_6D_6	< 2 (@ 1 MeV)
GNEIS	Russia	40	-	5% (@ 100 MeV)
nELBE	Germany	4	C_6D_6 + BaF_2+Li-glass (18% ^6Li)	~1

To improve the energy resolution, it is necessary to increase the base L.

With an increase in L, the counting rate in the recorded time spectrum decreases.

It is necessary to look for the optimum. In this case, the scintillators should not limit the temporal resolution.

GAGG для регистрации нейтронов высоких энергий: ToF

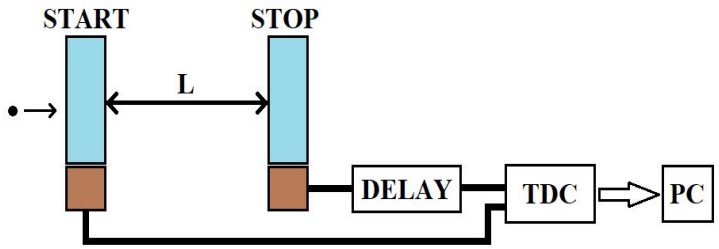

Связь между энергетическим и временным спектрами:

$$F(E) = \varphi(t)\frac{1}{m}\frac{t^3}{L^2}\left(1-\frac{L}{ct}\right)^{2}\frac{3}{2}$$

Нерелятивистский случай:

$$E_n = \frac{mv^2}{2} = \frac{mL^2}{2\tau^2}$$

Релятивистский случай:

$$E_n = mc^2\left(\frac{1}{\sqrt{1-\frac{1}{c^2}\left(\frac{L}{\tau}\right)^2}}-1\right)$$

Энергетическое разрешение vs временное разрешение:

Нерелятивистский случай:

$$\frac{\Delta E}{E} \sim \frac{\sqrt{E}}{L}\Delta t$$

Релятивистский случай:

$$\frac{\Delta E}{E} \sim \frac{1}{L}\sqrt{\gamma}\left(\gamma+2\right)^{\frac{3}{2}}\Delta t$$

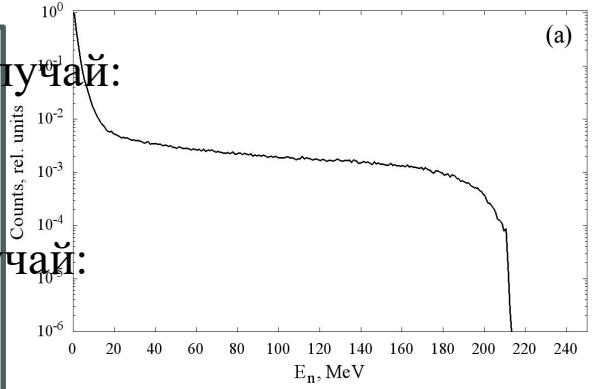

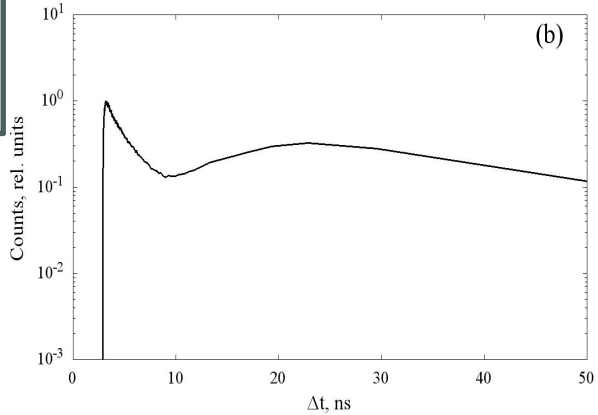

Смоделированный энергетический спектр F(E) нейтронов (а) и соответствующий ему

GAGG для регистрации нейтронов высоких энергий: ToF

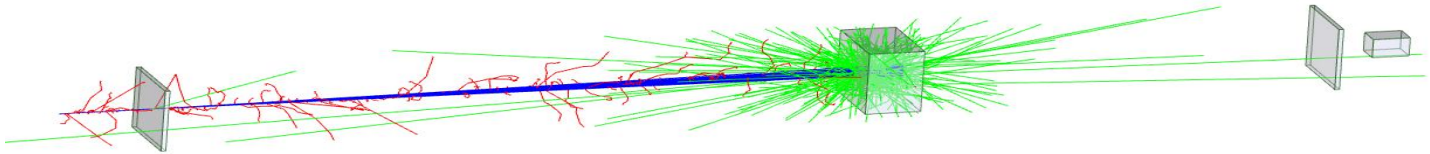

Схема проведения эксперимента

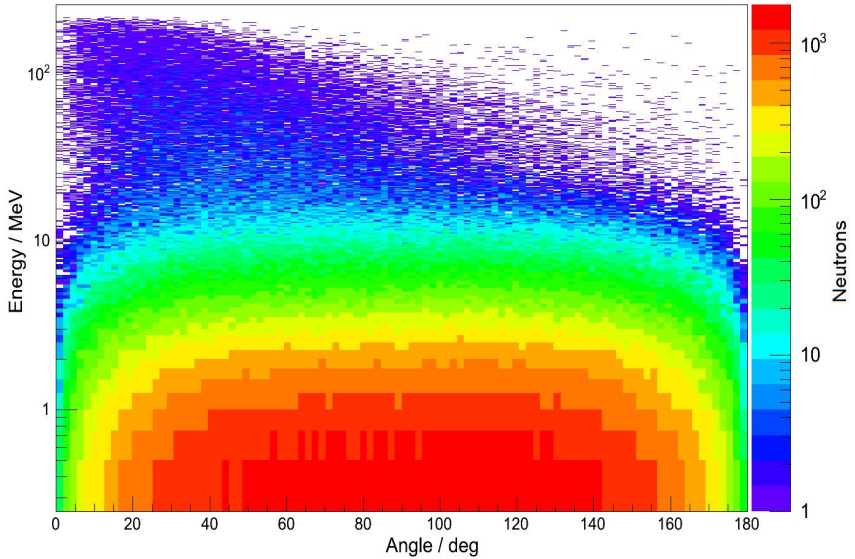

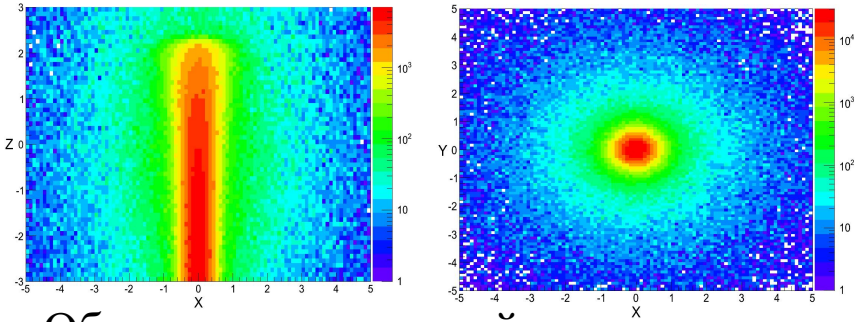

Область генерации нейтронов в свинцовой мишени

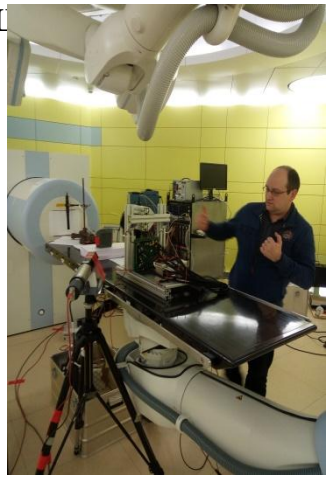

Смоделированное распределение нейтронов по энергиям и углам вылета за пределы свинцовой мишени размером 10×10×6 см. Нейтроны образуются в результате реакции (p,n) в мишени, E_p = 220 МэВ, углы определены относительно начального направления пучка протонов.

ToF experimental setup: preliminary modeling

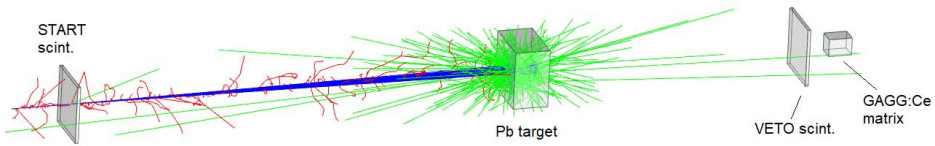

Fraction of particles falling from the Pb target to the detector at different bases L @ E_{p+}=220 MeV:

L, m	neutrons N/N_0, %	Gamma N/N_0,%	t_γ, ns	t_n, ns
0,25	0.25	0.04	1.5	2.5
0,5	0.07	0.01	2	4
1	0.02	0.003	4	7

Region of neutron generation in the target:

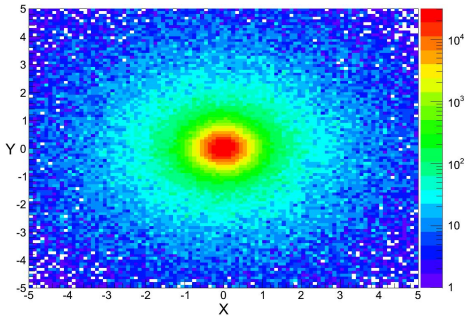

front view

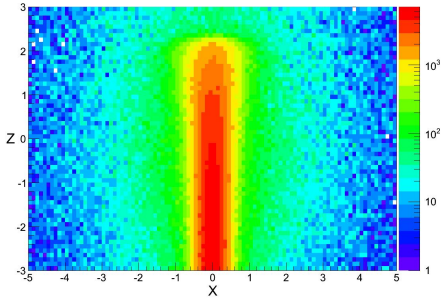

side view

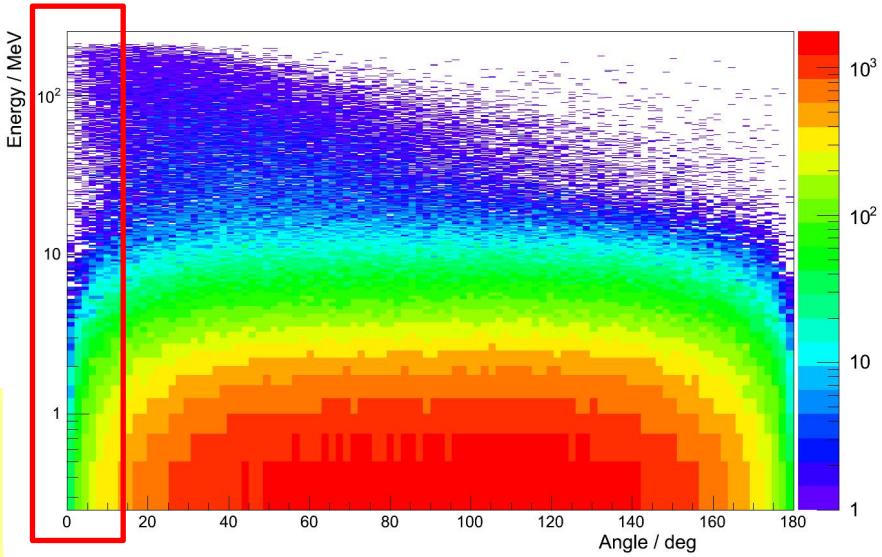

Expected energy and angular distribution of neutrons emitted from the Pb target @ E_{p+}=220 MeV

Modeling results:

- Optimal target - 60 mm of Pb
- Optimal distance at which it is possible to separate n and γ - 0.5 m

ToF experimental setup with an accelerator neutron source

Marburg Center for Ion Beam Therapy (MIT, Marburg, Germany):

- proton energy 220 MeV
- Pb(p,xn)X: neutron spectrum in the energy range up to 200 MeV and γ-quanta up to 10 MeV

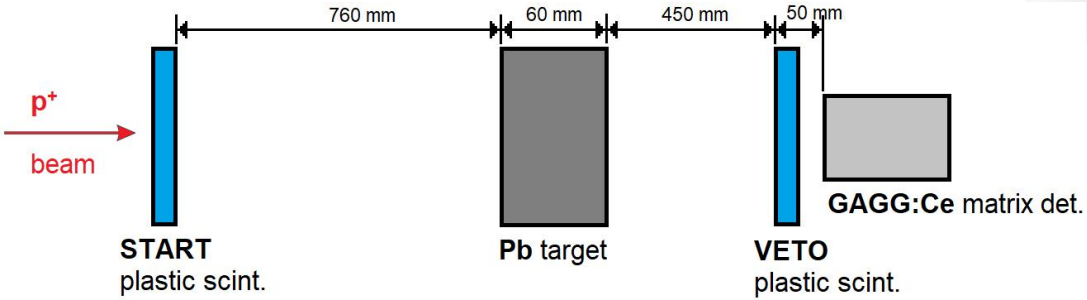

GAGG matrix: 64 crystals 3×3×40 mm

SiPM matrix photo detector: 8×8 SiPMs 3×3 mm

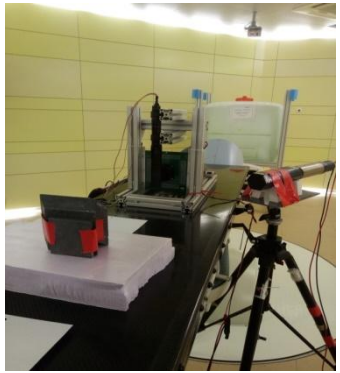

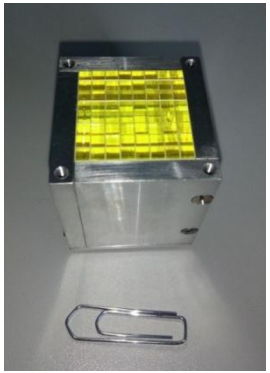

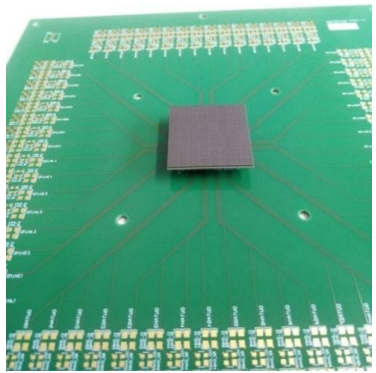

ToF experimental setup: results

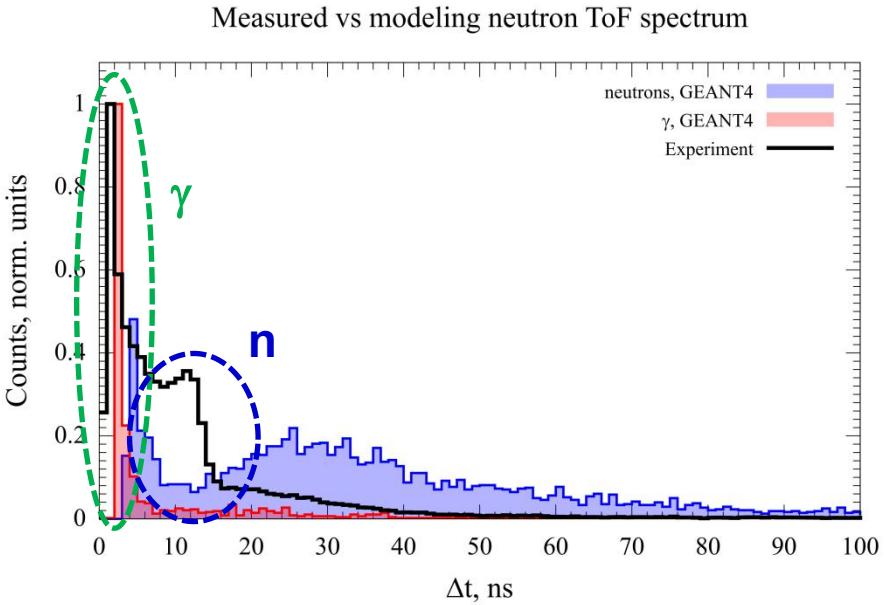

Experimental ToF spectrum vs modeling spectra for neutrons and γ

- The first 20 ns of the spectrum show two peaks corresponding to γ-quanta and fast neutrons.
- The time-of-flight spectrum generally confirms the results obtained in GEANT4 simulations.
- Estimation of the time resolution of the used setup: $\Delta t = 1.0$ ns.

Preliminary reconstruction of the neutron energy spectrum:

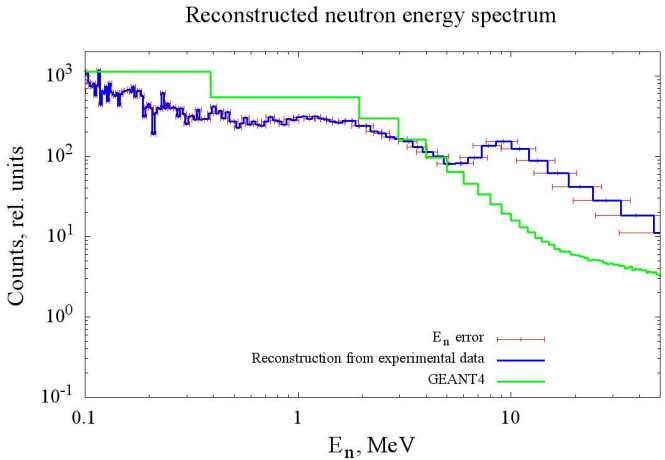

- GAGG allows to detect neutrons in a wide energy range with sufficient efficiency.
- GAGG doesn't limit the time resolution on small bases.
- Due to the high efficiency of gamma quanta registration GAGG can simultaneously act as a neutron detector. This makes it possible to implement the ToF method based on a single channel, which detects the prompt gamma-quanta + neutrons (distributed in time due to the base-of-flight).

ToF experimental setup: multiplicity registration

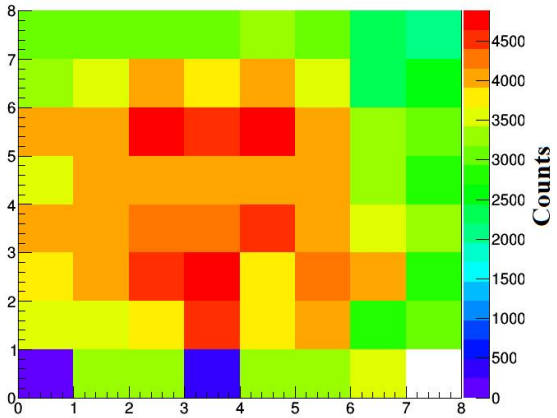

Response of GAGG matrix pixels on neutron registration

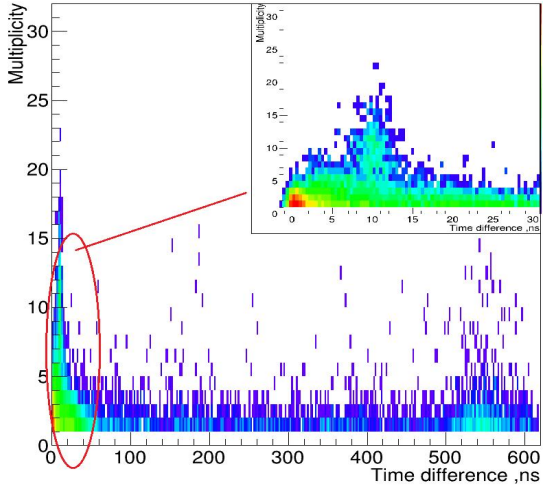

Dependence of multiplicity vs time of flight

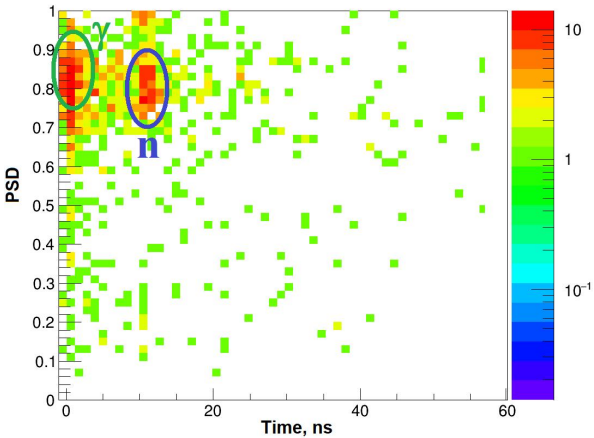

Dependence of PSD vs time of flight

In Gd-based scintillators a unique possibility of using multiplicity is realized using pixelated detectors:

- helps to search for events corresponding to a cascade of γ-quanta;
- proves the presence of two areas in the first nanoseconds in ToF spectrum;
- allows to distinguish the response from neutrons of different energies;
- opens the possibility of n/g discrimination without timing.

Thank you for your attention!

Questions?

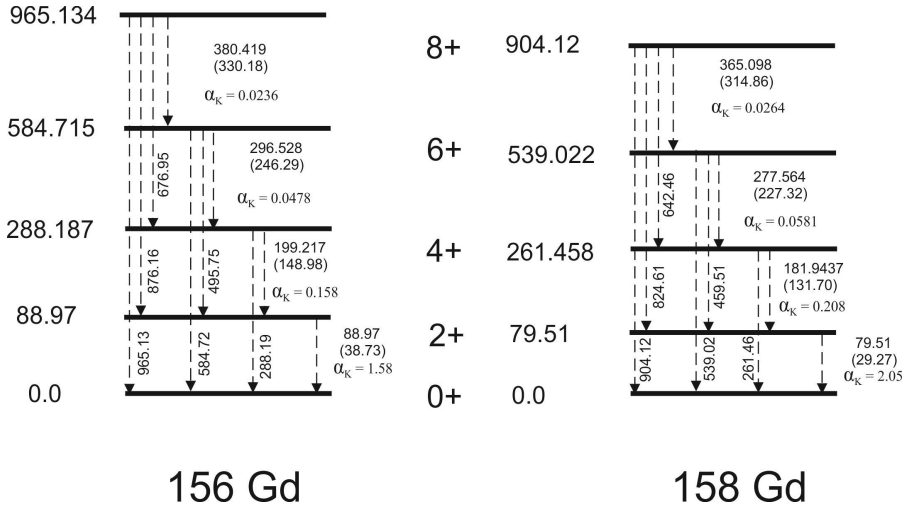

156 Gd

158 Gd

Изотопный состав природного гадолиния

Изотоп	Сечение взаимодействия с тепловыми нейтронами, барн	Содержание в природном Gd, %
^{152}Gd	739.76	0.2
^{154}Gd	86.0	2.18
^{155}Gd	60991	14.8
^{156}Gd	1.799	20.47
^{157}Gd	254840	15.65
^{158}Gd	2.222	24.84
^{160}Gd	1.424	21.86